Università degli Studi di Salerno

Facoltà di Scienze
Matematiche, Fisiche, Naturali
Dipartimento di Chimica e Biologia

Dottorato in Chimica
(X Ciclo)

Functionalized Syndiotactic

Polystyrene

Tutor: **PhD Student**
Ch.mo Prof.   **Rosa Califano**
Vincenzo Venditto

2008-2011

I

INDEX

Chapter 1: Introduction

Chapter 2: Materials and Experimental methods 20

Results and discussion: PART I - Sulfonation

Results and discussion PART II – Chloromethylation

List of abbreviatons

- s-PS: Syndiotactic Polystyrene
- a-PS: Atactic Polystyrene
- DCE: 1,2-Dichloroethane
- VOCs: Volatile Organic Compounds
- SEM: Scanning Electron Microscopy
- EDS: Energy dispersive spectroscopy
- CMOE: Chloromethyloctylether
- FTIR: Fourier Transform Infrared
- TGA: Thermogravimetric analysis
- GPC: Gel Permeation Chromatography

Abstract

The synthesis of polymeric materials by modification method, to obtain the desired properties in polymers, is an important topic in polymer chemistry and technology. Quite often, desired properties are not achievable by a single homopolymer. A strategy commonly used to obtain this purpose is the anchoring of specific functional groups along the polymer chains

In this context the interest in the functionalization of syndiotactic polystyrene (s-PS) arises, a semi-crystalline thermoplastic polymer that has low cost and excellent mechanical and dielectric properties, excellent heat and solvent resistance. In addition, the sPS has a complex polymorphism and the peculiarity that two of his note crystalline forms are nanoporous and are characterized by the presence of empty spaces (cavities in the δ-form and channels in the ε form) within the crystal lattice, able to accommodate small molecules.

This thesis presents new selective functionalization strategy only for amorphous phase of s-PS that at the same time does not change the crystalline phase and therefore all the characteristics of the s-PS.

In particular, in Chapter 3 the sulfonation of s-PS films and their characterization is reported.

The sulfonation allows to introduce a polar acid group on the polymer chains of s-PS amorphous phase, which makes hydrophilic the polymer, with a capacity of proton exchange. From

here the idea of using sulfonated films of sPS as polyelectrolytic membranes in fuel cells.

In chapter 3 are reported proton conductivity and the capacity to absorb water from the sulfonated sPS films at varying sulfonation degree. It was also well described the behavior of sulfonated s-PS films after the Fenton's test. In Fenton's test membranes are exposed to drastic oxidizing conditions, similar to those that develop in fuel cells. The ability of sulfonated s-PS films to resist the oxidizing conditions of Fenton test while maintaining good values of conductivity, reveals a possible practical application of this material as polyelectrolytic membrane in fuel cells.

The addition of hydrophilic properties on the polymer amorphous phase has the additional effect of improving the properties of sPS nanoporous crystalline phases to absorb VOCs from aqueous environments.

Indeed, it is expected that hydrophilic amorphous phases rapidly absorb aqueous solutions containing organic compounds, VOCs, making these ones (usually nonpolar) more easily available for the sorption in crystalline nanoporous phases of sPS.

In Chapter 4, the sulfonation of s-PS aerogels and their characterization are reported. In particular we have studied the sorption kinetics of a molecule model (1,2-dichloroethane, DCE that is representative of VOC category), from dilute aqueous solutions (50-100 ppm), in the nanoporous δ phase of sPS sulfonated aerogels at varying sulfonation degree. The data indicate that the sulfonation only of the amorphous phase of s-PS

increases the sorption kinetics of DCE. This behavior suggests potential practical use of sPS sulfonated aerogels systems for the purification of water or air from volatile organic compounds.

In Chapter 5 the chloromethylation of sPS δ-films and their characterization are reported.

The introduction of chloromethyl groups on the polymer chains of s-PS amorphous phase allows to obtain a highly versatile polymer that by simple nucleophilic reaction with appropriate reagents can give numerous other functionalized polymers.

In this regard, the amination reaction of chloromethyl sPS is shown. The aminated polymer contains another polar group with anion exchange capacity. This property, limited to the amorphous phase, allows to use aminated sPS semi-crystalline membranes as anion exchange membranes in fuel cells.

Moreover, the anionic conductivity and the capacity to absorb water by aminated sPS membranes are reported. These membranes show a good ability to absorb water and a good anionic conductivity.

Finally it should be noted that the characterization of functionalized s-PS samples (sulfonated, chloromethylated, aminated), performed by infrared spectroscopy and X-ray diffraction, indicates that the presence of functional groups only in the amorphous phase leaves essentially unchanged the crystallinity and the orientation of the nanoporous δ crystalline phase of the sPS, up to high degrees of functionalization.

In conclusion, the proposed functionalization techniques allow to increase the properties and applications of s-PS respecting to the already known features of the polymer.

Chapter 1: Introduction

1.1.Functionalization of polymers

The synthesis of polymeric materials by modification method, to obtain the desired properties in polymers, is an important topic in polymer chemistry and technology [1,2]. Quite often, desired properties are not attainable by the properties of a single homopolymer [3], but physical, chemical and mechanical desired properties of polymers can be obtained by anchoring some functional groups [4]. In this regard a variety of reactions have been employed for the chemical modification of polymers and for the synthesis of typical functional polymers such as ion-exchange [5] resins and photoresists [6].

Recently various functional polymers, namely, polymer-supported catalysts, polymer-supported reagents, polymeric photosensitizers, photoresponsive polymers, solar energy storege-exchange polymers and polymeric drugs, have become of great interest to scientists and engineers [7].

These polymers can be ordinarily prepared by different methods.

- Polymerization of the desired functional monomers: the monomer unit is functionalized first and then proceed with its polymerization.

- In situ functionalization: the main monomer unit is copolymerized with other functionalized polymers, or during the polymerization of

the main monomer, adding a functionalizing agent that can act as chain-transfer.

- Post-polymerization functionalization: by chemical modification of the polymer, in solution or directly on the solid.

Direct polymerization of functional monomers is the preferred method for effectively introducing the functional groups into the polymer chain. However, there are some problems and limitations in the processes of synthesis, purification, and selective polymerization of monomers containing functional groups. Its also very difficult to control the distribution of functional groups in the polymer chain when the functional monomers are copolymerized with other monomers containing no functional groups.

Although a complete and quantitative introduction of the functional groups into the polymer chain is possible by previous method (polymer reaction), the post-polymerization functionalization method is extremely convenient for obtaining a number of functional polymers because many organic reactions can be employed.

In general post-polymerization modification is based on the direct polymerization or copolymerization of monomers bearing chemoselective handles that are inert towards the polymerization conditions but can be quantitatively converted in a subsequent step into a broad range of other functional groups [8].

The synthesis of functional polymers through post-polymerization modification is schematically illustrated in Scheme 1.1.
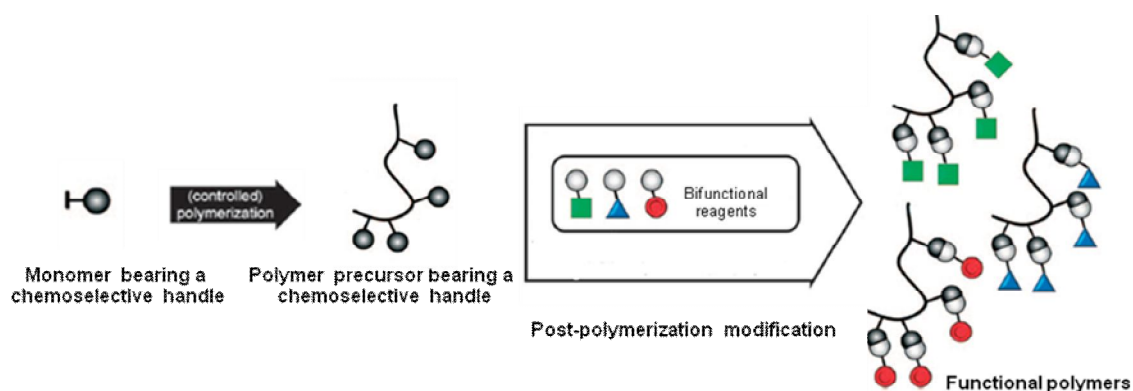
Scheme 1.1. *Synthesis of polymers by post-polymerization modification*

The success of this method is based on the excellent conversions achievable under mild conditions and the excellent functional-groups tolerance.

Moreover, as shown in Scheme 1.2, most of commercial polymers can be utilized as starting materials, this makes the post-polymerization modification a method even more attractive.
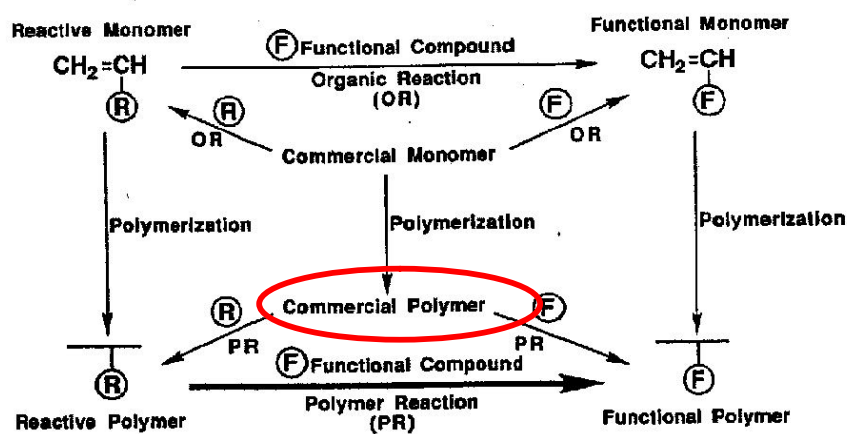
Scheme 1.2.

1.2. Syndiotactic polystyrene (s-PS)

Syndiotactic polystyrene (s-PS) is a promising semi-crystalline engineering plastic that was synthesized for the first time 20 years ago [9]. Its fast crystallization rate, around two orders of magnitude greater than isotactic polystyrene, enables its use as raw material for plastic industry. The excellent balance between mechanical and dielectric properties, solvent and heat resistance confers high potentialities to its applications.

Its relatively low cost combined to such properties has motivated the commercialization of this material by Dow Chemical Co. (QuestraTM) and Idemistsu (XarecTM) together with a substantial interest of the scientific community [10]-[14].

Several drawbacks can however restrict its practical use as performance plastic. s-PS has to be processed at high temperatures, greater than 290°C, due to its melting point of 270°C, which approaches its degradation temperature. The brittleness of s-PS can be detrimental in areas where mechanical properties are of prime importance. The lack of polar groups may also disfavor its use in applications where adhesion and compatibility with other polymers are required.

The introduction of functional groups in s-PS may help to overcome these drawbacks.

However s-PS presents a very complex polymorphic behavior and exists in different morphologies, all this makes even more interesting this material and its modification.

1.2.1. Polymorphism of syndiotactic polystyrene

Structural studies have shown that, s-PS, exists in five crystalline forms named α, β, γ, δ, ε, which differ in the conformation of the polymer chains (conformational polymorphism) and the packing of the chains in the unit cell (packing polymorphism).

The α and β crystalline forms are characterized by polymer chains in the trans-planar conformation with a repetition period of 5.1 Å [15].In the α form the chains are packed to form a hexagonal type unit cell [16], while the crystalline structure of the β form is of orthorhombic type [17].

Both α and β forms may have different degrees of structural order dependent on the preparation and treatment conditions. In particular, one can obtain two limit order modifications (α″,β″) and two limit disordered modifications (α′,β′).

The two polymorphic forms, γ, δ, ε are characterized by chains in helical conformation with symmetry s(2/1)2 and a repetition period of 7.7 Å [18].

In the δ form the chains are packed in a monoclinic unit cell, while the crystalline structure of the γ form has not yet been resolved [17b].

Recently it was discovered a fifth crystalline form, named ε, which is characterized by chains in helical conformation [18a].

A

B

(a)

5.1 Å

7.7 Å

(b)

trans-planare (α,β)

eliche s(2/1)2 (γ,δ,ε)
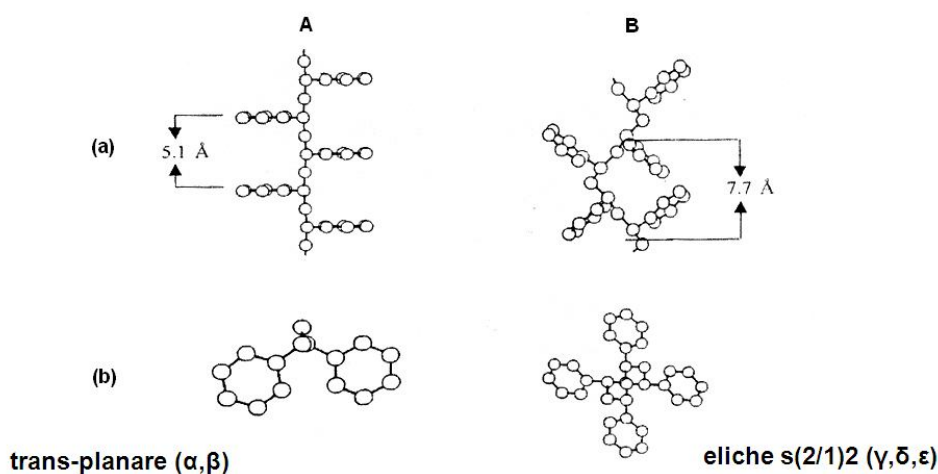
Figure 1.1.: *Projection of the s-PS in trans-planar conformation (A) and helical conformation (B). Both the projections are in a plane containing the chain axis (a) and in a plane perpendicular to the chain axis (b).*

The δ and ε forms of s-PS present a nanoporous crystalline structure due of the presence of empty spaces able to accommodate a great number of guests. In particular the δ-form is characterized by the presence of cavities, while the ε-form is characterized by the presence of channels.

Starting from the δ and ε nanoporous structures, co-crystalline phases of s-PS with low molecular mass molecules can be obtained [19]. The inclusion of one guest molecule for each cavity forms clathrate structures, while the inclusion of guest molecules layers between layers of enantiomorphic helices of the polymer forms intercalate structures.

The two trans-planar chains (α and β forms) can be obtained from melt processing or vitreous samples subjected to thermal treatments [16].

Instead the three helical chains with a s $(2/_1)2$ (forms γ, δ and ε) can be obtained from solution-processing [16].

In figures 1.2 and 1.3 are summarized these processing.

Polymorphism and melt-processing
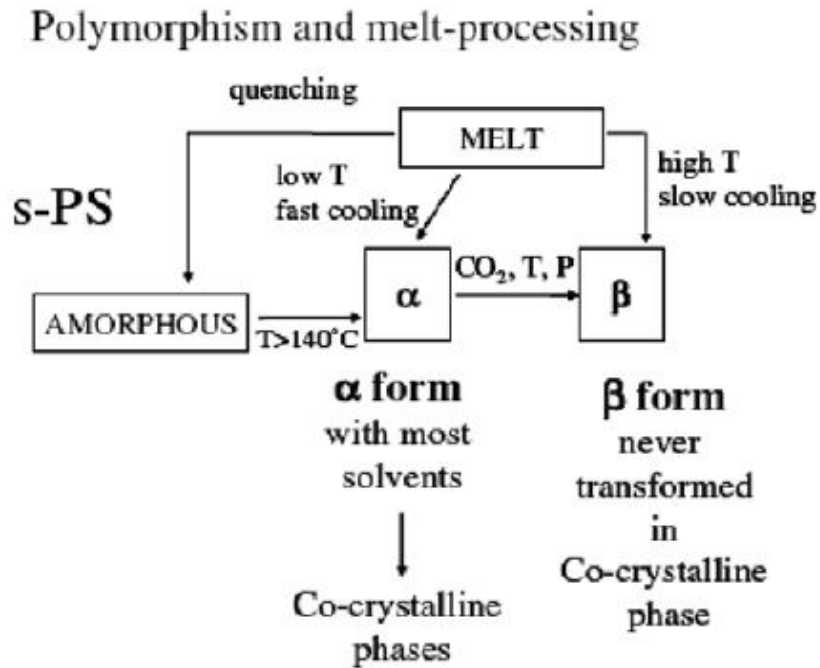
Figure 1.2.: Schematic representation of the main crystallization and interconversion conditions for the various phases of s-PS obtained by melt-processing.

Polymorphism and solution-processing
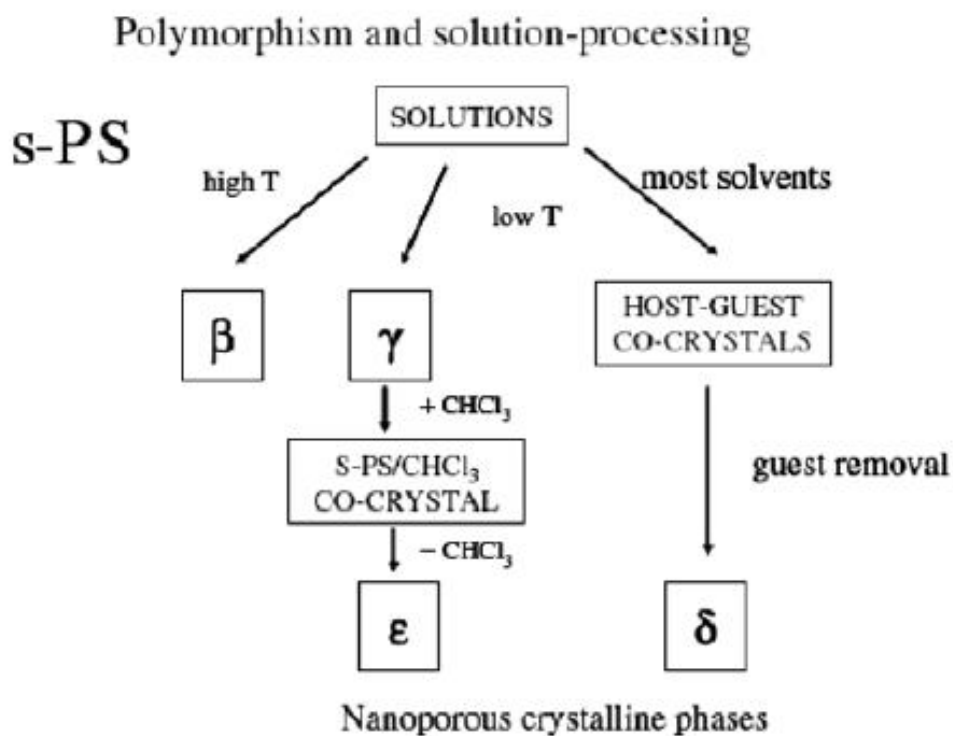
Figure 1.3.: *Schematic representation of the main crystallization and interconversion conditions for the various phases of s-PS obtained by solution-processing.*

As shown in Figure 1.2 and Figure 1.3, the β form can not generate co-crystalline phases, while the α form can form co-crystalline phases with most solvents. However the δ and ε forms are more suitable for the formation of co-crystalline phases of s-PS and are achieved by solution crystallization processes.

In Figure 1.4 the X-ray diffraction patterns (obtained with an automatic diffractometer) with the corresponding Miller indices of samples disoriented in all crystalline forms, are shown.
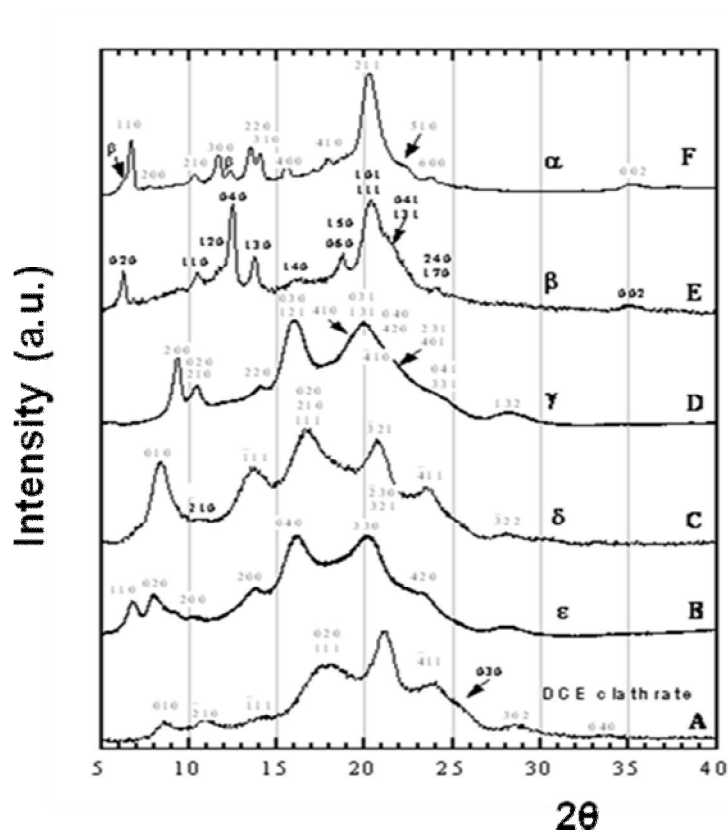
Figure 1.4.: *X-ray diffraction profiles of the five crystalline forms (α, β, γ, δ, ε) of s-PS compared with a s-PS/1.2-dichloroethane chlatrate sample.*

1.2.2. The δ crystalline form

The δ form of s-PS is a nanoporous structure, that presents cavities arising from packing of polymer chains.

For the presence of these nanometric cavities, δ form of s-PS, is able to accommodate guest molecules of suitable size and shape

giving rise to clathrate structures [20], that are different for each guest molecule and for lattice parameters of cell.

Uptake selectivity of guest molecules depends on the polarity, the size and shape of the cavity.

The guest molecules can be absorbed from vapor or liquid phase and can be, for example, halogenated compounds (chloroform, dichloromethane, etc), aromatic compounds (benzene, toluene, etc.), cyclic compounds (cyclohexane, tetrahydrofuran), but also inorganic molecules such as titanium tetrachloride.

Removing the guest molecules from clathrates the nanoporous form can be obtained.

The guest molecules can be removed by different procedures, for example, extraction with low-boiling solvent (CS_2, acetone), or by extraction with carbon dioxide in supercritical conditions. The first procedure involves the exchange of the guest molecule with other molecules more volatile, the latter forming unstable clathrates, and guests go away from the polymer by simple exposure to air, leaving the empty nanoporous form of s-PS.

However, the faster and more efficient procedure for emptying is that one which uses CO_2 supercritical conditions [18]; moreover the CO_2 is also not toxic, is cheap and easily it has accessible critical parameters (Tc = 31 ° C and Pc = 73 atm). Few hours of treatment with supercritical CO_2 are necessary for the complete substitution of the guest molecules and just a few minutes of exposure to the air are needed to remove the CO_2 absorbed by the polymer and to obtain a sample in the nanoporous δ form.

1.2.3. Volume and size of the cavities in the δ form.

In the crystal structure of the δ form, the polymer chains, in helical conformation, are packed in a monoclinic unit cell (with lattice constants a = 17.4 Å, b = 11.85 Å, c = 7.7 Å and $γ$ = 117°, space group P2$_1$/a) containing two isolated cavities.
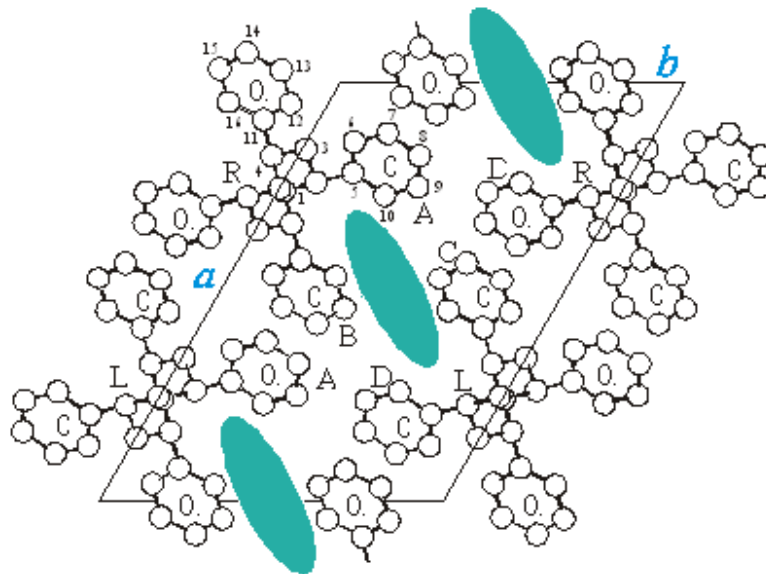
Figure 1.5.: *Representation of the cavities characterizing the crystalline phase of the δ form of s-PS. Each crystalline cavity is confined by 10 host phenyl rings. R right-handed; L left-handed helices.*

The volume and size of the cavities in the δ form of s-PS were evaluated by adding spaces in the crystal structure able to contain hypothetical spheres of radius 1.8 Å, which is a typical value of the Van der Waals radius of an atom of chlorine or a methyl group. The volume of the cavities thus obtained is about 125 Å^3 [21].

In Figure 1.5. the projection along the c axis and the perpendicular projection to the ac and bc planes in two unit cells of

the form δ, are shown. In addition in the shade is outlined, the region of empty space corresponding to a cavity divided between two cells.
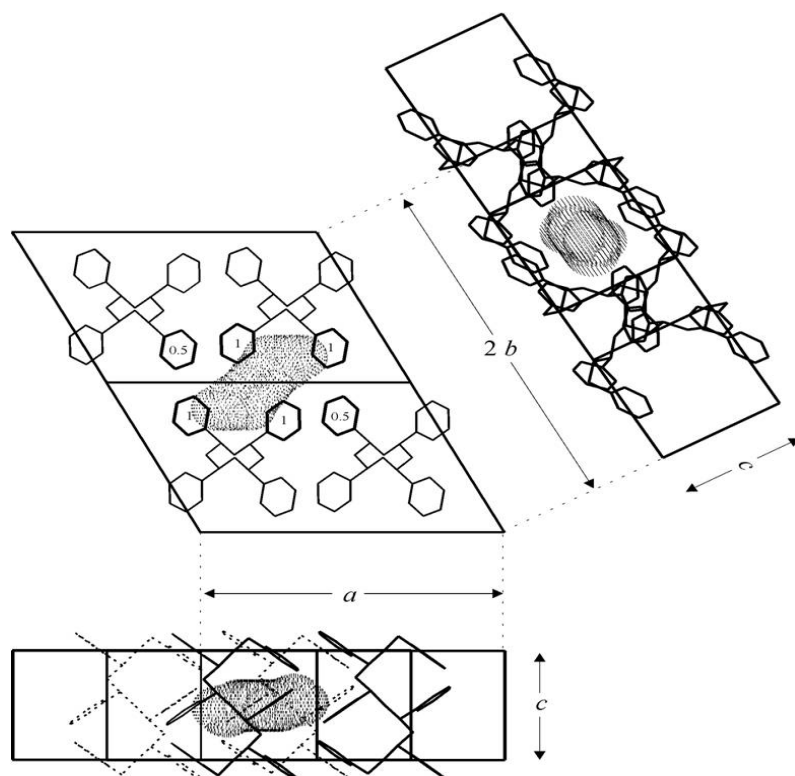
Figure 1.6.: *Packing model proposed for the crystal structure of the unit cell in the form δ. It's shown the projection along the axis and the perpendicular projection to the planes ac and bc. In shade, the cavities in the crystal lattice are shown.*

Figure 1.6 shows the empty space corresponding to that cavities that are found in the center of symmetry in the crystal structure, bounded by ten phenyl rings.

After the formation of clathrates each cavity is occupied by a guest molecule, (except for the clathrate with iodine (I_2) [19], in which there are two guest molecules per cavity).

With the formation of clathrates, the size of the unit cell (and the volume of the cavity) become higher than those observed in the case

of the nanoporous δ form. In presence of a guest, an extension of the axis *b* and the distance *bsenγ* are verified, which corresponds to the distance between the rows of chains parallel to *a* axis.

1.2.4. The β crystalline form

The β form [17] is the only stable crystalline form to the solvents and also the thermodynamically most stable form of s-PS due to better packing of polymer chains, which is achieved in its cell.

The β form is the most dense crystalline form of s-PS [22]; in fact its density (ρ = 1.03 g/cm3), is about 20% higher than the density of the δ form (ρ = 0.997 g/cm3).

1.2.5. Crystalline clathrate forms of s-PS

Clathrate crystalline forms are obtained by treatment of samples of s-PS, in the form α and γ, with suitable solvents, or induced by the crystallization of amorphous samples.

The δ-clathrates of s-PS can be divided into two different classes: monoclinic and triclinic [23].

In particular, monoclinic δ-clathrates are obtained with guests whose molecular volume is significantly lower to that one of the cavity of the δ nanoporous crystalline phase ($\approx$0.125 nm^3). In these monoclinic δ-clathrates the guest molecules are easily accommodated in the cavities of the δ phase, essentially only assisted by a possible increase of the distance between the *ac* layers of closely packed enantiomorphous polymer helices (d_{010}), thus maintaining a monoclinic unit cell and the P2$_1$/a symmetry of the

nanoporous δ form. Moreover, in the monoclinic δ-clathrates, the molecular planes of planar guest molecules assume an orientation perpendicular to the chain axes.

Because, in most cases, a single guest molecule is present in each cavity, the maximum molar ratio between guest molecules and styrenic units is 1/4.

On the other hand, triclinic δ-clathrates are obtained with guests whose molecular volume is significantly higher than that one of the cavity of the δ nanoporous crystalline phase ($\approx$0.125 nm^3).

As example, for the triclinic δ-clathrate with 4-nitroaniline (NA) having a guest with a volume similar to the cavity volume of the δ phase, and showing only a minor increase of the d_{010} spacing, NA molecules are accommodated in all the isolated cavities of the δ phase, mainly by shifting the *ac* layers along the chain axis, thus leading to a triclinic (rather than monoclinic) unit-cell and to guest molecular planes inclined with respect to the helical chain axes (Figure 1.7B).

In figure 1.7 the distortion of unit cell from monoclinic with p-nitrobenzene guest (A) to triclinic with p-nitroaniline guest (B), is reported

$d_{010} = 1.12$ nm $d_{010} = 1.08$ nm

R   L   R   L

c   c

b+a/2   b+a/2

(A)   (B)
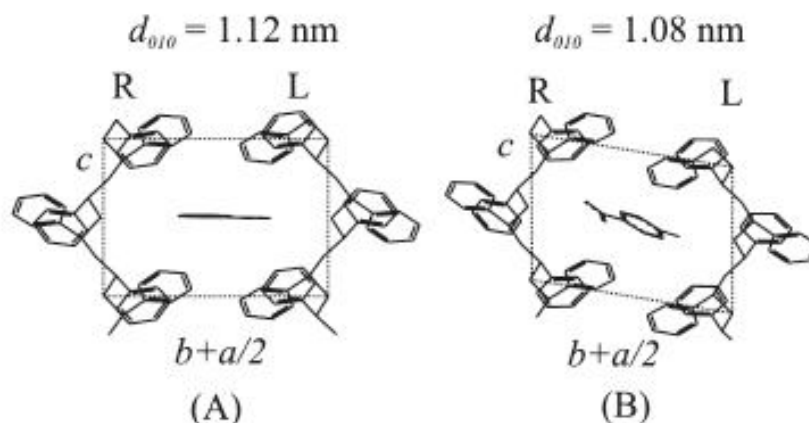
Figure 1.7.: *Packing model proposed for the δ-clathrate structures of s-PS with p-nitrobenzene (A, monoclinic) and p-nitroaniline (B, triclinic). Only a couple of enantiomorphous polymer helices (R=right-handed;L = left-handed) that confine the guest molecule is shown. A closer distance between the ac layers is observed for the bulkier p-nitroaniline guest (B) because the guest is rather accommodated by shifting the ac layers along the chain axis, leading to the triclinic symmetry.*

Also in this case the maximum molar ratio between guest molecules and styrenic units is 1/4.

Indeed in triclinic δ-clathrates with bulky guests, the close packing of the polymer chains along in the *ac* layers is partially lost and one-half of the cavities initially presents in the δ phase is lost while the other one-half increases its volume and becomes suitable to host bulky guest molecules. This of course halves the maximum guest/monomer-unit molar ratio that becomes 1/8.

Finally, guest molecules having a volume similar to the cavity volume of the δ phase present a more complex behavior. In these cases, in order to establish to which one of the two classes the clathrate belongs, it is important to determine the d_{010} spacing. In particular, for d_{010} spacing similar or lower than that the δ

nanoporous crystalline phase clathrate structure are expected to be triclinic while for d_{010} spacing decidedly higher the structures are expected to be monoclinic. This is reflected in X-ray diffraction spectra, in fact the position and relative intensities of different reflections vary depending on the guest.

As example in **figure 1.8** X-ray diffraction patterns of some δ-clathrate with different guest molecules are reported.
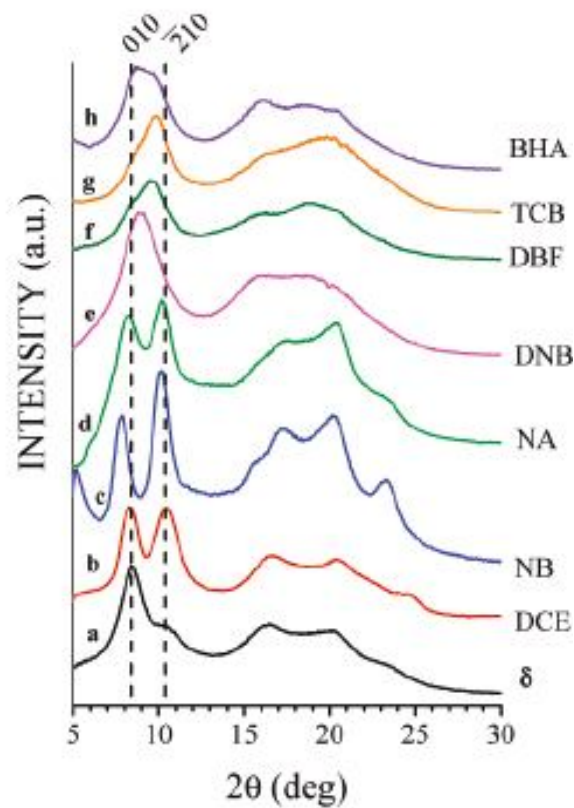
Figure 1.8.: *X-ray diffraction patterns of s-PS uniaxially oriented films exhibiting crystalline or cocrystalline phases: (a) empty δ; δ-clathrate with (b) dichloroethane (DCE),(c) nitrobenzene (NB), (d) p-nitro-aniline (NA), (e) 1,4-dinitro-benzene (DNB), (f) dibenzofuran (DBF), (g) 1,3,5-trichlorobenzene (TCB), and (h)2-tert-butyl-4-methoxyphenol (BHA). (A) The positions of the 010 and 210 reflections 010 of the nanoporous δ form indicated with dashed lines.*

The position of the first reflection at $2\theta \approx 8°$ is particularly indicative for the *b*-axis dimension (reflection 010); increasing the size guest this reflection (010) becomes progressively smaller (ie the axis b extends and expands the unit cell) and shifts to higher values of 2θ.

1.3. Morphology of syndiotactic polystyrene

Besides to the specific characteristics described above, the morphological aspect makes, the s-PS and in particular its δ crystalline form even more interesting. In fact, you can easily process the polymer in order to obtain products of appropriate forms (powders, films, pellets ect..). More recently s-PS was, also, obtained as aerogels.

1.3.1. Aerogels of Syndiotactic Polystyrene

Aerogels are generally defined as a class of materials characterized by highly porous network and very low density, which consist mainly of air (over 95%) and a small fraction of the solid matrix.

Although aerogel preparation methods have been marked by several breakthroughs since the 1930's, most aerogels produced so far are characterized by chemically bonded three-dimensional networks [24, 25].

High porosity s-PS aerogels exhibiting physically bonded three-dimensional networks have been obtained by supercritical CO_2

extraction of the solvent present in s-PS physical gels [26] or by sublimation of the solvent [27].

As an example, figure 1.8 shows that the dimensions of a s-PS gel prepared in chloroform at a polymer concentration C_{pol}=0.10g/g remain substantially unchanged during the extraction procedure [26a].
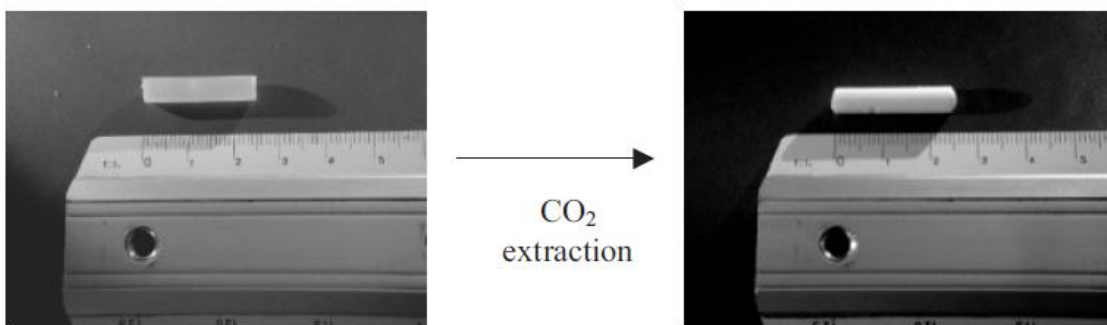
Figure 1.8.: photographs of a piece of sPS gel prepared in chloroform C_{pol}=0.10g/g, before and after complete chloroform extraction by supercritical CO_2 extraction.

s-PS aerogels are highly porous manufacture (until P=98.5%), which is characterized by low density and high surface area, all this makes the aerogels unique class of materials, being attractive for many applications such as thermal and acoustic insulation or catalysis.

The crystalline phase of the aerogels as well as their morphology depend on the crystalline structure of the junction zones of the starting gel, and by using suitable techniques can be well controlled [28]. In particular, the crystalline structure can be nanoporous (δ or ϵ) as well as dense (β or γ).

In literature is reported that aerogels obtained from sPS/chloroteadecane gels present the β crystalline phase, while aerogels obtained from sPS/chloroform gels present the δ crystalline phase. Typical X-ray diffraction patterns of β and δ forms aerogels are shown in figures 1.9 a and c respectively. In figure 1.9 is also shown that β aerogels (figure 1.9 b) present interconnected lamellar crystals with thickness in the range 200-400 nm, while δ aerogels (figure 1.9 d) present a fibrillar network morphology with fiber diameters of the order of 50-100 nm. The latter consists of macro pores (between nanofibrils) and micro pores (into nanofibrils) [28].
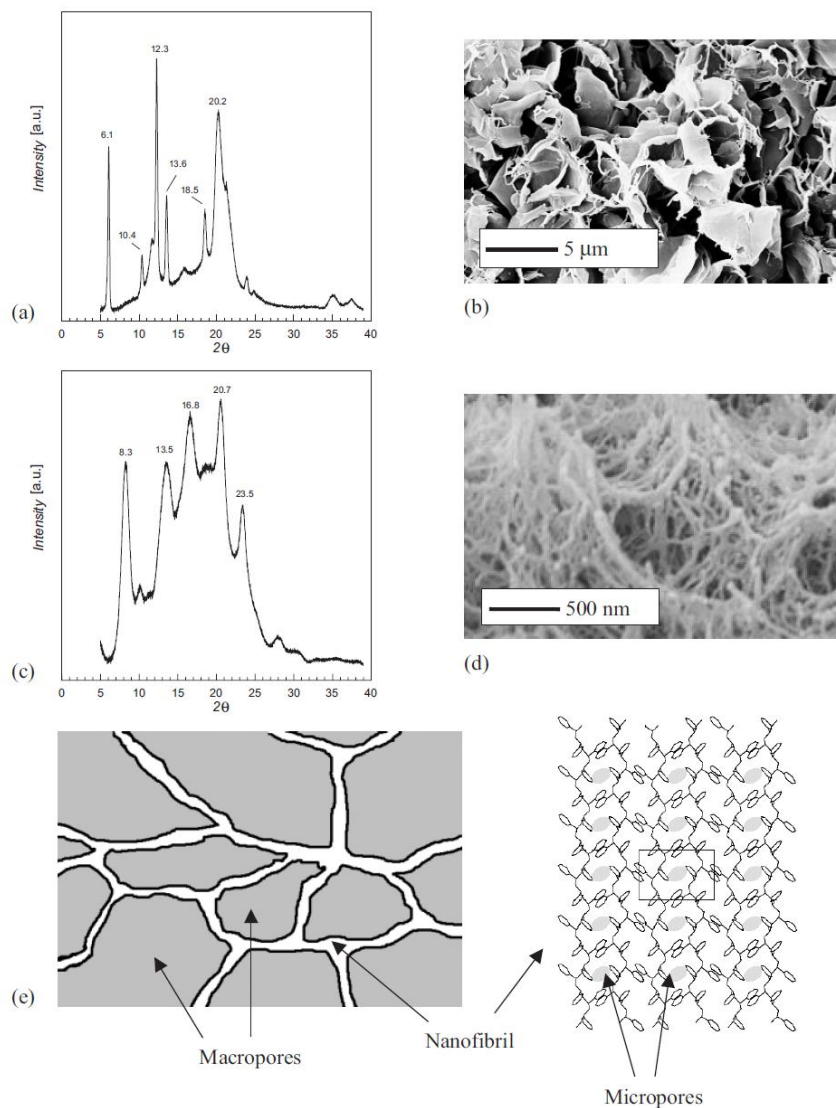
Figure1.9.:*X-ray diffraction patterns and electron micrograph of s-PS obtained from gels prepared in chlorotetradecane (β aerogels, (a,b)) and chloroform (δ aerogels, c,d). e) Schematic presentation of the texture (left) and of the crystalline structure (right ; the nanocavities are shaded) of the δ-aerogels*

Syndiotactic polystyrene aerogels have attracted even more interest because, as shown in a recent paper [29], it presents sorption kinetics of volatile organic compounds (VOCs), from dilute

aqueous solutions, much faster than the corresponding films. In particular the δ form s-PS aerogel presents this behavior due to the nanoporous crystalline phase.

Chapter 2: Materials and experimental methods.

The s-PS used in this study was manufactured by Dow Chemical Company under the trademark Questra 101. The 13C nuclear magnetic resonance characterization showed that the content of syndiotactic triads was over 98%. The weight-average molar mass obtained by gel permeation chromatography (GPC) in trichlorobenzene at 135°C was found to be Mw=3.2 $\times$105 with the polydispersity index, Mw/Mn=3.9.

Solvents and reagents used had been provided by Aldrich and used as such without further purification processes.

2.1 Preparation of δ crystalline form s-PS samples

2.1.1. Preparation of δ crystalline form s-PS films

In this thesis were used δ form s-PS films obtained by crystallization from solution (casting).

The casting is a molding technique which consists the payment of a solution of the polymer in a Petri dish and allow to evaporate the solvent at the required temperature. In particular, a solution used was 0.5% by weight of s-PS in chloroform. The thickness of the samples depends on the diameter of the Petri dish, the concentration and amount of solution used.

2.1.2. Preparation of δ crystalline form s-PS aerogels

All s-PS aerogel samples were obtained by treating sPS/chloroform sulfonated native gels with a SFX 200 supercritical

carbon dioxide extractor (ISCO Inc.) using the following conditions: T = 40 °C, P=200 bar, extraction time t =180 min).

All native s-PS gel samples were prepared in hermetically sealed test tubes by heating the mixtures above the boiling point of the solvent until complete dissolution of the polymer, and the appearance of a transparent and homogeneous solution had occurred. Then the hot solution was cooled to room temperature where gelation occurred.

2.2. Determination of functionalization (sulfonation, chloromethylation) degree by elemental analysis.

The functionalization degree (S, Cl) is reported as the ratio of moles of sulfur and carbon atoms of the styrene units. This way of reporting the functionalization degree does not take into account the fact that only the benzene rings of amorphous phase of the polymer are functionalizated, as the mild functionalization conditions do not allow you to attack the compact crystalline phase. To know the real degree of functionalization on the amorphous phase, it is necessary to know the degree of crystallinity (Xc) of each sample and use the relationship:

Functionalization degree of amorphous phase = functionalization degree of polymer$/1$-Xc

Admitting that functionalized s-PS samples have a constant crystallinity of 40%, to know the functionalization degree on the amorphous phase the above formula becomes:

27

$$S = \frac{(moliS)}{(moliC)} x1.66$$

However during this thesis, the degree of functionalization will be reported only as the ratio of moles of sulfur and carbon atoms of the styrene units.

2.2.1. Elemental analysis: *instrumentation*

The instrument used for the elemental analysis experiments is the FlashEA 1112 THERMO.

The technique for the determination of C, H, N, and S is based on "dynamic flash combustion". The sample is weighed into a tin capsule and placed in the sampler of instrument, which is washed by a flow of helium and then dropped in a vertical quartz reactor, maintained at a temperature of 1020 ° C (combustion reactor).

When the sample falls into the combustion reactor, at the flow of helium is temporarily add pure oxygen, the sample and the tin capsule melt and causes a violent reaction (flash combustion). Under these conditions, each type of substance is completely oxidized. The combustion is then made quantitative by passing the gas mixture through an oxidation catalyst. The gas mixture is then passed over a layer of metallic copper wire to remove the excess oxygen and reduce nitrogen oxides to elementary nitrogen. After the mixture is sent to a cromatrografic column where the individual gases are separated and eluted as nitrogen, carbon dioxide, water and sulfur

dioxide. A thermal conductivity detector generates an electrical signal proportional to the concentration of the element you want to determine.

2.3. FTIR spectroscopy

The infrared spectra were obtained with a Tensor 27 Bruker spectrometer, equipped with a DTGS detector and a beam splitter to the Ge / KBr. The spectra were registered in a frequency range from 400 to 4000 cm^{-1} with a resolution of 2 cm^{-1} and 16 scans that were performed to improve the signal to noise ratio.

The FTIR spectroscopic analysis has allowed us to have useful information on the sulfonated films and aerogels of s-PS. It was possible:

• to study the conformation of the polymer chains and obtain the crystal structure

• determine the orientation of polymer chains in the crystalline phase

• evaluate the absorption of molecules by analyzing the bands related to the guest molecules absorbed.

The degree of crystallinity, calculated from FTIR measurements, is expressed as mole fraction Xc and is calculated using the formula K = l/l'(1-Xc) [21-22], where K is the coefficient of removal, l and l'are respectively the thicknesses of the sulfonated films of s-PS and amorphous reference sample.

2.4. X-ray diffraction

The structural investigation of sulfonated film was made through X-ray diffraction measurements (RX). With this technique it is possible to obtain qualitative and quantitative information on the type of crystalline phase, its degree of crystallinity and the orientation of crystallites in space.

The spectra were obtained using an automatic diffractometer Bruker D8 Advance, which uses copper Kα radiation filtered with a Ni filter. RX diffraction profiles were registered in the range 2θ: 4 ° -40 °, while scanning with step of 0.05 ° with acquisition times of 3 seconds per point.

By examining the RX spectra is possible to calculate the correlation length (D010) of the crystalline domains using the Scherrer formula:

$$D_{hkl} = 0.9\lambda / \beta_{hkl} \cos\theta_{hkl}$$

β_{hkl} where is the width at half height expressed in units of radians, λ is the wavelength of the incident radiation and θ_{hkl} is the amplitude of the diffraction angle.

2.5. Scanning Electron Microscopy.

The instrument used is the Leica Cambridge Stereoscan 440.

The basis of scanning electron microscopy (SEM) consists of an electron beam generated by an electron gun (cathode), the beam is attracted toward the anode, condensed by collimating lens and focused onto the sample through objective lenses . The electron

beam hits the sample, producing secondary electrons and back scattered.

These electrons are collected by a detector for secondary electrons and back scattered electrons for one, their signal converted into electrical signals and amplified, so these signals are converted to pixels and processed by a computerized system, which provides the image.

2.6. Energy dispersive spectroscopy

The X-ray energy dispersive spectroscopy, (X-ray EDS) is a technique associated with scanning electron microscopy (SEM).

The technique uses X-rays emitted from the sample during bombardment with an electron beam that characterizes the composition of the element analyzed. When the sample is bombarded by the electron beam of the SEM, the electrons were expelled from the surface of the film and this form a gap that is subsequently occupied, by an electron to a higher energy level. X-radiation is emitted to balance the energy difference between the two electrons. The X-ray EDS detector measures the number of X photons emitted as a function of their energy, which is characteristic of the element analyzed. In this way qualitative and quantitative information, on the elements present in the sample can be obtained.

2.7. Extraction by supercritical CO2

Samples of functionalized s- PS were treated with a supercritical CO_2, utilizing an instrument called SFX 200 extractor

(ISCO Inc.) set to the following conditions: T = 40 ° C, P = 200 bar and extraction time of 3 hours for films and 6 hours for aerogels. The pressure and temperature at which the behavior of supercritical CO_2 shows are 73.8 atm and 31.1 ° C.

2.8. Determination of water absorption

The water uptake was evaluated using a thermogravimetric analyzer Q5000 SA, which is equipped with a microbalance, in which the sample is in a room with controlled temperature and humidity. All measurements are performed under a nitrogen stream at 200 ml per minute.

2.9. Determination of proton conductivity

Proton conductivity of membranes was determined from lateral resistance of membranes that was measured using a four-points-probe electrochemical impedance spectroscopy technique .

The cell was equipped with two platinum foils outer current-carrying electrodes and two platinum wires inner potential-sensing electrodes. The inner electrodes had a diameter of 0.8 mm and were placed at a distance of 0.42 cm. Impedance measurement was performed using a Solartron SI 1280B electrochemical impedance analyzer. The instrument was used in galvanostatic mode with AC current amplitude of 0.01 mA over a frequency range from 0.1 to 20000 Hz. The complex impedance was reported in Bode plots with log frequency on the x-axis and both the absolute value of the

impedance and phase-shift on the y-axis. The resistance of samples was obtained using the absolute value of the impedance in the frequency range where it was approximately constant and the phase angle was close to zero. Then, the proton conductivity σ was calculated using the equation:

$$\sigma = \frac{L}{R \times A}$$

where R is the resistance value extracted by Bode plots as described above, L is the distance between the inner electrodes and A is the cross-sectional area of the membrane.

Before measurement, membrane samples were cut into strips approximately 1.0 com wide, 2 cm long and 0.02 cm thick and immersed in distilled water for 2 hours at room temperature. Then it was blotted and mounted in the Conductivity Cell.

2.10. Thermogravimetric analysis

The thermogravimetric (TGA) analysis were conducted by a NETZSCH 290 F1 analytical balance (0.01 mg precision).

The thermogravimetric analysis allows to obtain information on changes in the mass of the samples when heated. In fact it is possible to determine the presence of volatile compounds, the decomposition temperature of the sample, the content of inorganic residue.

Thermogravimetry records the change in weight of a sample as a function of temperature, which varies linearly once fixed the heating rate. the instrument used for analysis consists of a thermobalance is a accurate balance placed inside a furnace at controlled atmosphere (nitrogen or air). the sample is placed on the scale to zero after the weight of the capsule. By heating the sample is degraded and the degradation products are removed from a gas stream, while the software records weight changes.

Chapter 3 Sulfonated Syndiotactic Polystyrene

As mentioned above, syndiotactic polystyrene (s-PS) is a robust polymeric material with high melting point, high chemical stability and high crystallization rate [9]. The possible use of sulfonated s-PS as

proton conductive membranes for fuel cells.[37] have been recently reported in literature. These studies describe sulfonation procedures in solution, leading to random sulfonation of the polymer chains and hence strong reduction of crystallinity and related chemical and thermomechanical resistance.

In this chapter we show that, exploiting (both for the processing and the final material properties) the complex polymorphic behavior of s-PS, highly crystalline membranes can be achieved, which exhibit a thermal and chemical-resistant unsulfonated crystalline phase and a proton conductive sulfonated amorphous phase.

s-PS nanoporous films were sulfonated using the innovative technique [38]. which takes advantage of the molecular selectivity of nanoporous δ phase of s-PS. This technique provide a sulfonation in heterogeneous phase by treating the polymer films with chloroform, which is able to form a co-crystalline structure with the host s-PS nanoporous δ phase and an appropriate sulfonating agent previously prepared.

The selective sulfonating agent is particularly bulky and therefore it is unable to enter into the nanoporous crystalline phase. At the same time the chloroform solvent is able to easily penetrate both into amorphous phase and into the nanoporous crystalline phase, so that polymeric film is rapidly swelled. The sulfonating agent mobility, inside the swelled film, is facilitated and the sulfonation only of amorphous phase becomes rapid and uniform.

3.1. Sulfonation procedure

The δ-form s-PS films used for the sulfonation procedure have been obtained by casting from 0.5 wt% solutions in chloroform, at room temperature.[18] The films present uniplanar orientation [18c] of co-crystalline phases and thickness in the range 40-60 μm.

The acyl sulfate, sulfonating reagent, was prepared by mixing at room temperature an excess of dodecanoic acid (lauric acid) over chlorosulfonic acid

$$CH_3(CH_2)_{10}COOH + ClSO_3H \rightarrow CH_3(CH_2)_{10}COOSO_3H + HCl$$

sulfonating reagent
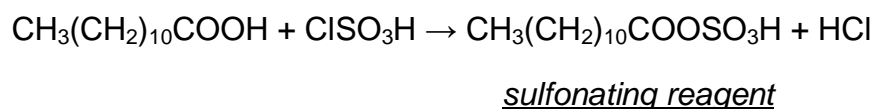
In particular 1.6 mol of lauric acid (≥98%, Aldrich) was used per 1.0 mol of ClSO₃H (99%, Aldrich) and the reaction was conducted in Nitrogen atmosphere for 24 hours. All reagents were used as received.
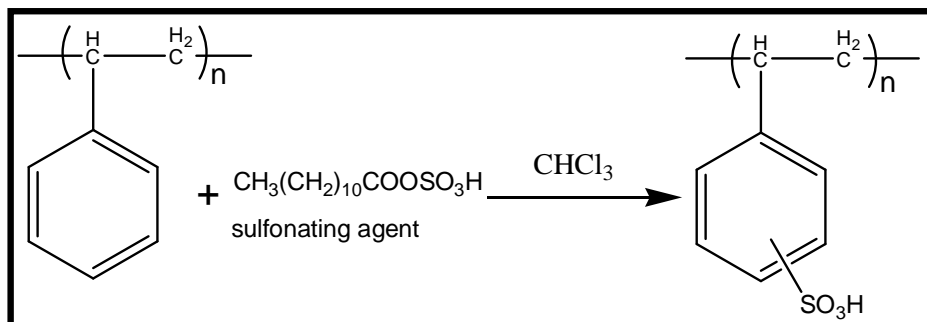
Scheme 3.1: *Sulfonation reaction*

Aftert the sulfonation of s-PS films, exhibiting the nanoporous δ phase, was performed at temperature of 40°C, by soaking the films in acyl sulfate solution in $CHCl_3$ (99%, Aldrich).

The sulfonated films, have been purified by possible remnants unreacted chemicals by washing with ethanol and then extracting with carbon dioxide in supercritical conditions, with a SFX 200 supercritical carbon dioxide extractor (ISCO Inc.), by using the following conditions: T= 40°C, P = 200 bar, extraction time t = 180 min. As well established in the literature,[39] the extraction with carbon dioxide in supercritical conditions allows complete removal of possible guest molecules from s-PS co-crystalline phases, leading to nanoporous crystalline phases.

3.1.1. Optimization of sulfonation procedure

In order to obtain s-PS films with different sulfonation degree, reactions were performed by varying the concentration of the sulfonating reagent solution, initially, and then the reaction time. In

particular solutions with concentrations of 0.1M, 0.05M have been used and reaction time was varied from 1 to 24 hours.

It's worth mentioning that this optimized procedure has high reproducibility.

The **table 3.1**. shows the results obtained for the experiments conducted in different sulfonation conditions:

Sample	Reaction time (min)	Concentration (M)	% S atoms/styrenic units
1	20	0.1	30
2	30	0.1	45
3	40	0.1	15
4	90	0.1	40
5	120	0.1	42
6	10	0.05	5
7	15	0.05	9
8	20	0.05	17
9	30	0.05	22

Table 3.1: *Sulfonation degree (determined by elemental analysis) of some nanoporous δ s-PS film achieved in different sulfonation condition.*

3.2 Characterization of sulfonated nanoporous s-PS films
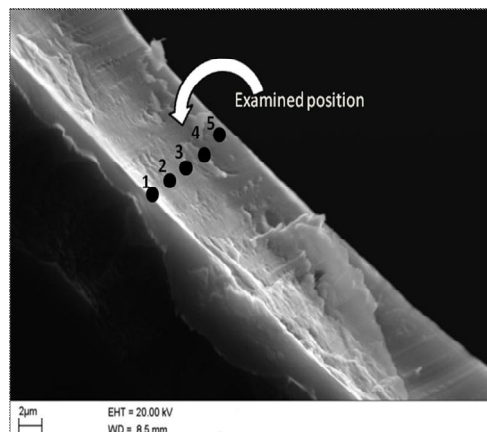
3.2.1 SEM Analysis

In order to verify the sulfonation uniformity all along the sample sections, the films were examined with a scanning electron microscope (SEM) coupled to a probe EDS (energy dispersive spettroscopy). As an example, in figure 3.1. a SEM micrography of the film section of sample 8 is shown. In **table 3.2**. the content of sulfur for each point examined by EDS probe (**figure 3.1**. labeled in 1-5) is shown.

Figure 3.1: *Scanning electron microscopy images of the section of naoporous δ s-PS film (sample 8). The black dots indicate the examined points by EDS profiling analysis.*

Examined position	molS/molC x 100
1	19
2	17
3	12
4	8
5	11

Table 3.2: *values of sulfur in each position examined by SEM microscopi coupled to a probe EDS, for sample 8*

The values of the % S, ranging from 11 to 19, indicate that the sulfonation procedure described above for δ-form s-PS film leads to an efficient and uniform sulfonation.

3.2.2 FTIR characterization

Infrared characterization of sulfonated s-PS films gives informations about sulfonation degree and allows us to evaluate the crystallinity of film.

The s-PS film used for the sulfonation had a thickness between 50 and 70 microns to be easier to handle however, we observed that even for thin films, in which the degree of sulfonation is higher than 3%, most of infrared bands present absorption values too high to be readable. The saturation of absorption peaks is due to the-SO3H groups and ionic bonds having very broad infrared bands.

In fact FTIR spectrum has many unreadable areas in which the values of absorbances are too high to be reliable.

In **figure 3.2.** the FTIR spectra, in the region 1450 e 1420 cm^{-1}, of some δ-form s-PS films at different sulfonation degree are shown.
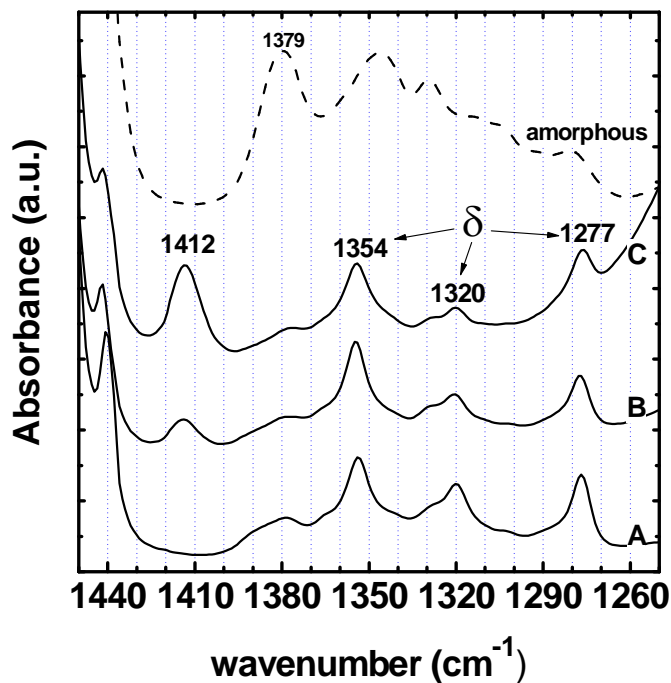
Figure 3.2: FTIR spectra in the wavenumber range 1450-1250 cm-1 of s-PS film with nanoporous crystalline δ-phase, (A)) before and (B-C) after sulfonation procedures. Relevant absorbance peaks associated with the crystalline (1354, 1320) phase or with the sulfonation level (1412 cm-1) are also indicate.

In **figure 3.2**. we can see that after sulfonation the peak at 1412 cm^{-1} appears. The intensity of this peak increases with sulfonation degree.

In a recent paper a linear dependence between the value of sulfonation degree and the 1412 cm^{-1} peak intensity value, has been observed. An evidence of this behavior is shown in **figure 3.3** where

the absorbances at 1412 cm-1, normalized respect film thickness *vs* the sulfonation degree values, determined by elemental analysis are reported**.**
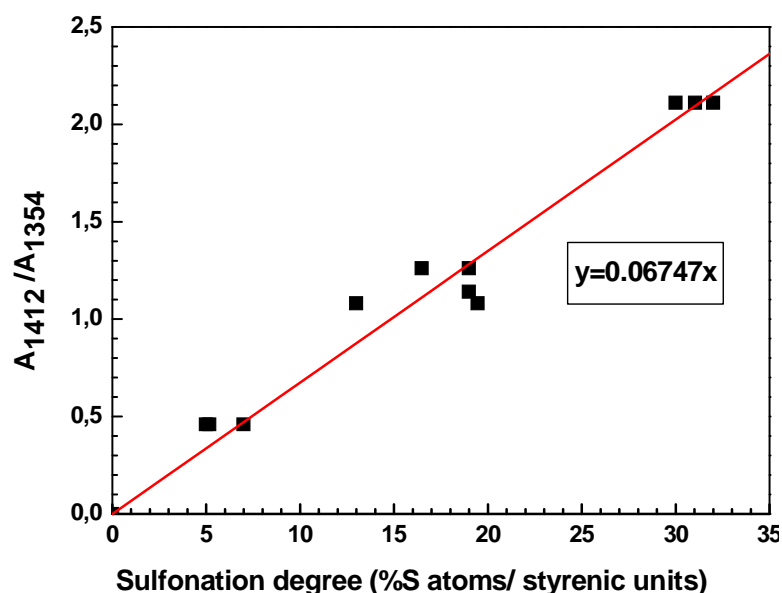
Figure 3.3: *relationship between the absorbance of 1412 cm^{-1} peaks and sulfonation degree evaluated by elemetal analysis.*
Absorbance of 1412 cm^{-1} peaks was normalized respect
absorbance of 1354 cm-1 , latter is correlated at film thickness.

According with this liner relationship the intensity of the 1412 cm^{-1} peak, normalized respect to film thickness, was considered to be representative of the sulfonation degree of achieved sPS samples and infrared absorbance measurements was used for determining sulfonation degree values instead of elemental analysis.

Moreover in the FTIR spectra of **figure 3.2.** the typical peaks of sPS δ crystalline phase, that are located at 1354, 1320 and 1277, are

present. These peaks are a clear evidence that the films retain the integrity of δ-crystalline phase after sulfonation procedure.

The degree of crystallinity (Xc), evaluated by subtracting the spectrum of a fully amorphous s-PS film and by reduction close to the baseline of the 1379 cm^{-1} amorphous peak, is resulted between 30 % and 50% corresponding to sulfonation degree between 5% and 40%.

3.2.3 RX characterization

The X-ray analysis allows us to obtain qualitative informations about δ-phase crystallinity and its orientation in sulfonated films.

In **figure 3.4**. the X-ray diffraction patterns of some s-PS δ-form films at different sulfonation degree are shown.
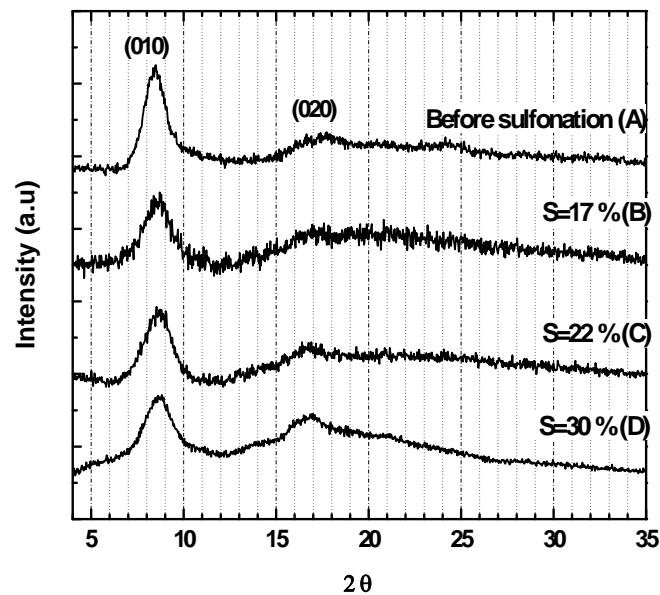
Figure 3.4: *X-ray diffraction patterns (Cu Kα) of s-PS films with the nanoporous crystalline δ-phase, before (A) and after (B-D) sulfonation procedures.*

The X-Ray diffraction patterns, show only (010) and (020) reflections, at 2θ CuKα ≈ 8.4° and 17° respectively. This pattern is typical of sPS films presenting the nanoporous δ phase and high level of uniplanar orientation.

A progressive increase in the intensity of the amorphous halo with the increase in sulfonation degree is also evident in **figure 3.4.**

However, the position and the intensity of the typical nanoporous δ phase peaks clearly show that the nature of crystalline phase(δ) and its uniplanar orientation are essentially unaffected by our sulfonation procedure, until at sulfonation degrees like to 30%.

The broadening of these peaks only indicates a slight reduction of the dimension crystals. In particular, the full width at half-maximum of the (010) peak , indicated as (β_{010}), is close to 1.2° for the unsulfonated film and increase up to 1.9° for the film with a degree of sulfonation of 17%.

3.3 Semicrystalline sulfonated s-PS films as proton-conductive membranes.

Ion-containing polymers (ionomers) are widely used as proton exchange membranes in fuel cells [40]. These membranes are generally exposed to very harsh environmental conditions, resulting from high local concentrations of acidic groups and from high operating temperatures, as well as from the oxidative conditions at the electrodes. Many industrially important ionomers, e.g. Nafion, are semicrystaline polymers, so that their desirable properties depend on the structure and morphology of the crystalline domains.

Syndiotactic polystyrene (s-PS) can be used as proton-conductive membranes because is a robust polymeric material with high melting point, high chemical stability and high crystallization rate.

3.3.1 Water uptake and proton conductivity of sulfonated δ–form s-PS films

The liquid water uptake and proton conductivity of s-PS sulfonated films having different sulfonation degree have been evaluated. In **figure 3.5**. liquid water uptake and proton conductivity versus the sulfonation degree are reported.
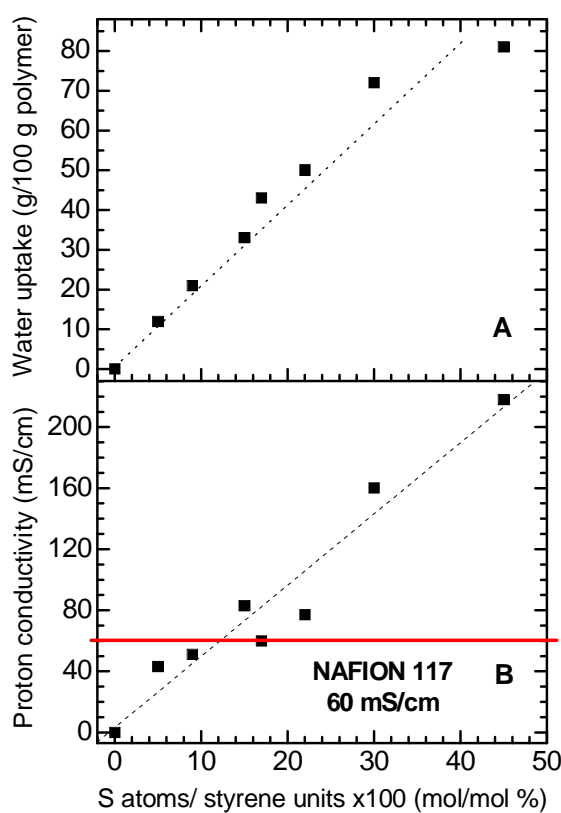
Figure 3.5: *Water uptake (A) and proton conductivity (B) at 31.5° and in liquid water of s-PS membranes, exhibiting the δ crystalline phase, as a function of the sulfonation degree (S). Lines are drawn to guide the eyes.*

In figure 3.5. both the water uptake and the conductivity are linearly dependent on sulfonation degree of s-PS films.

Moreover in **figure 3.5.B** is reported the value of Nafion conductivity, the polymer commonly used as poli-electrolytes membrane for fuel cells. Sulfonated s-PS membranes having proton conductivity higher than Nafion 117 have been achieved.

In **table 3.3**.a summary the properties of sulfonated s-PS δ-form films achieved during this thesis are reported.

Sample	% S atoms/styrenic units	Water uptake (%ww)	Proton conductivity (mS/cm)
1	30	72	160
2	45	81	218
3	15	33	83
6	5	12	43
7	9	21	51
8	17	43	60
9	22	50	77

Table 3.3: water uptake and proton conductivity of sulfonated δ s-PS membranes at different sulfonation degree.

3.3.2. Sulfonated β–form s-PS films

As already mentioned above working conditions of a fuel cell are very hard due to strong oxidizing and reducing reactions taking place at the anode and the cathode respectively. Moreover very strong acidity and basic conditions are associated to redox reactions. Finally, temperatures as high as possible would be preferable to maximize the reaction kinetics.

The δ-form of s-PS is thermally unstable and it may undergo structural changes of crystalline phase under the working conditions of a fuel cell, this makes it more susceptible to oxidation.

Hence the need arose to have a poly-electrolytic membrane suitable to work under these conditions, whereby we have tried to achieve the sulfonated s-PS membranes in thermodynamically stable β-form[41].

Attempts to achieve homogeneously sulfonated β-form s-PS films have not been successful. This is probably due to the fact that the dense and thermodynamically stable β crystalline phase is not permeable to the chloroform (solvent used), so that the sulfonating reactants are unable to diffuse in a bulk of film and the sulfonation is confined to thin surface layers.

We have verified that the β-form s-PS films absorbs less and slower chloroform than δ-form s-PS films. In fact the chloroform uptake of β-form s-PS films, after 1 hour of immersion in pure liquid, was only 2%, while the uptake for δ-form s-PS films was 34%.

Moreover for the latter, after 3h of immersion in pure liquid, the amount of chloroform was unchanged, instead for β-form s-PS films chloroform uptake was only 17%.

This behavior gives us understand that the failure of sPS β-films by our procedure is due to kinetic and thermodynamic reasons.

In fact, is clearly evident that the swelling time of the sPS β-film is very long than that observed for s-PS δ-film, this implies that the bulky sulfonating agent has thermodynamical difficulties to penetrate into the membranes. The last consequence is that the sulfonating

agent remains on the membrane surface causing the sulfonation only of the outer part of it.

However, in literature is reported that the δ phase of s-PS can be also transformed, by high temperature (210-250°C) annealing procedure, into β crystalline phase [18a]; this was our starting point to achieve sulfonated β-form s-PS membranes.

We have verified that, for sulfonated δ form s-PS samples swollen in water, the annealing procedure at T=210°C, induces δ→α transition, independently to the heating and cooling conditions.

The samples presenting β-phase can be achieved by a sudden annealing in the temperature range 230-250°C at sulfonated samples acetone swelled and followed by slow cooling at room temperature.

The oxidation resistance of the sulfonated β form membranes has been also explored by classical Fenton tests [42].

It's note that during the operation of fuel cells, cross-over oxygen from the cathode side, or air bleed on the anode side, provides the oxygen needed to react with hydrogen from the anode side and produce H_2O_2, which can decompose to give OH or OOH radicals.

These free radicals can easily attack any C–H bonds present in the polymer.

The attack of peroxide radicals on H-containing end groups is generally believed to be the principal degradation mechanism of non-fluorine PEM.

Up till now, Fenton test is still the most useful method to evaluate the chemical oxidation degradation of PEM.

Fenton test is a method to observe the changes of the membranes in a solution in which the hydroxyl (OH) and hydroperoxy (OOH) radicals are produced from the decomposition of H_2O_2 catalyzed by Fe^{2+}.

In present work the Fenton test was conducted with the following method: one piece of sulfonated β form s-PS membranes was immersed in a solution of H_2O_2 at 30% w/w containing 20 ppm Fe^{2+} (Iron sulphate, $FeSO_4.7\ H_2O$) at 80 °C (temperature at which fuel cell works) for 3 hours.

After Fenton test, in order to demonstrate the stability of membrane, proton-conductivity was evaluated. As for a membrane with S = 5%, the conductivity before and after Fenton test is slightly reduced from 43 mS to 41 mS.

Moreover after Fenton test, the changes of crystalline structure in β form s-PS membranes was also investigated.

In **figure 3.6**. the X-ray diffraction patterns of the membrane with a sulfonation degree of 5%, after annealing treatment are shown. In particular the pattern B corresponds to obtained s-PS α-film from sulfonated δ-film, by annealing at 240 °C into hot press, followed by fast cooling; the pattern C correspond to sulfonated s-PS β film obtained by annealing at 240 °C into hot press, followed by slow cooling (nearly 1°C/min) in the press and the pattern D correspond to sulfonated s-PS β-film after Fenton test.
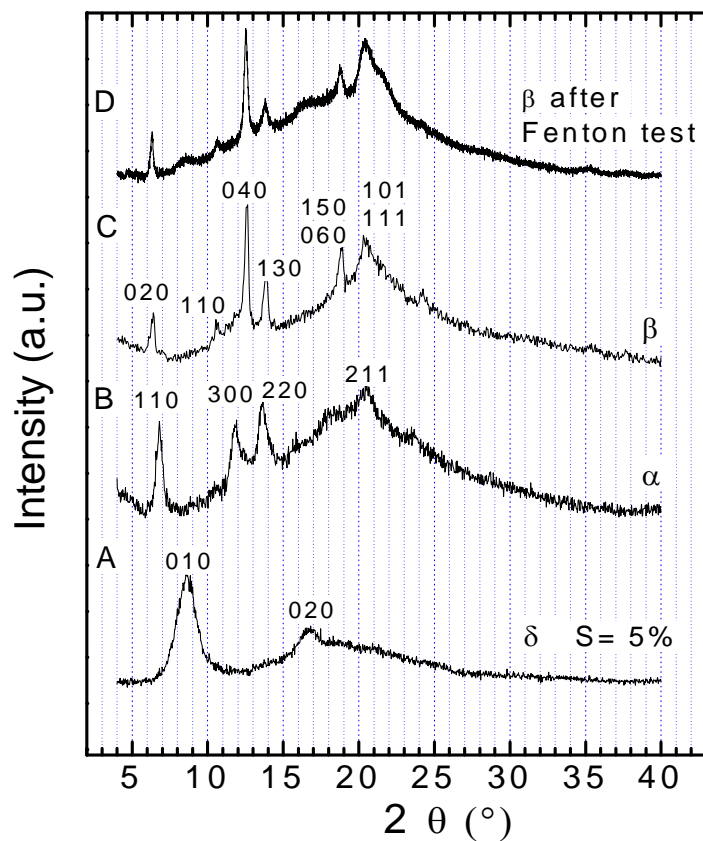
Figure 3.6: X-ray diffraction patterns of s-PS proton-conductive membranes exhibiting a degree of sulfonation S = 45% (A) and 5% (B-E). As for the latter membrane the different patterns correspond to (B) as prepared, δ form; (C) water swollen and annealed at 240°C, α form; (D) annealed at 240°C and slowly cooled, β form; (E) sample D after the Fenton test. The main peaks have been labeled by the Miller indexes of the reflections that characterize the crystalline phases.

In **figure 3.6** the relative intensities of the equatorial (hk0) and non-equatorial (hk1) reflections, of the patterns of B-C are analogous

to those reported for unoriented samples [16a][17a][18a] and indicate a substantial loss of orientation.

Moreover the high similarity between the X-ray diffraction patterns of C and D clearly indicates that the Fenton test has poor influence on the sample crystallinity.

In **figure 3.7**. the TGA curves of the β form membrane with a sulfonated amorphous phase (S = 5%) has compared with that one of unsulfonated β-form film are shown.
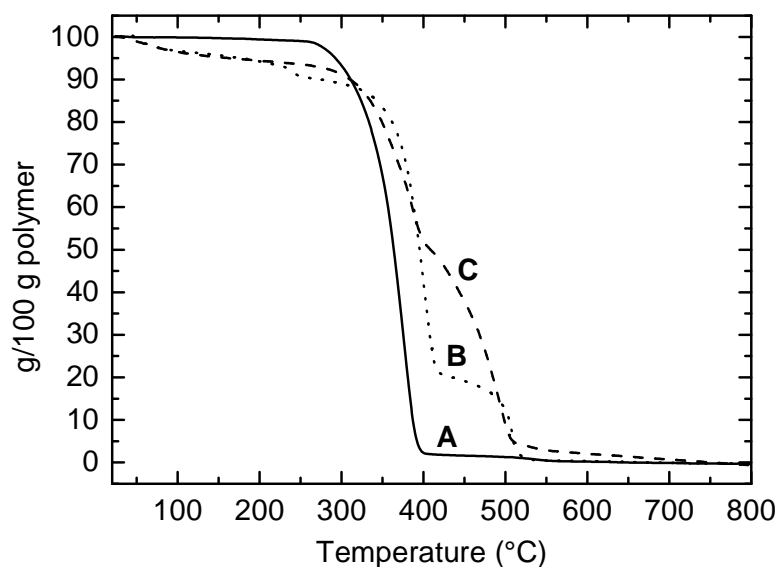
Figure 3.7: *TGA of s-PS proton-conductive membranes, exhibiting the β crystalline phase: (A) unsolfonated; (B) with a sulfonation degree S =5%; (C) with a S =5%, after the Fenton test.*

In **figure 3.7** it is possible to observe a similar loss of water for β film before and after Fenton test. The higher degradation temperature showed by the (B-C curves) possibly correspond to a partial cross-linking degree present in the sulfonated polymer. The comparison between the B-C curves shows that the membrane after Fenton test presents a substantially different degradation behavior only above 400°C.

3.4 Conclusions

In this chapter we have presented a solid-state sulfonation procedure, which if applied to s-PS samples exhibiting the nanoporous δ-crystalline phase allows an easy and uniform sulfonation of the amorphous phase phenyl rings.

X-ray diffraction and Fourier Transform Infrared measurements clearly show that the proposed sulfonation procedure is able to preserve the thermodynamically unstable nanoporous δ-phase, essentially also preserving its degree of crystallinity. By using this sulfonation procedure we were able to modulate the sulfonation degree of the polymer amorphous phase, at least up of 50% of phenyl rings of the polymer chains.

The sulfonic groups included on the polymer chains make the amorphous phase highly hydrophilic, but the crystalline phase remains preserved, which makes the polymer dimensionally stable.

Membranes based on sulfonated s-PS have shown proton-conductivity through their amorphous phases and a

thermomechanical stability due to their non-sulfonated crystalline phase.

Suitable thermal treatments on these s-PS sulfonated membranes can not lead only to the thermally stable α phase but also to the thermodynamically and chemically stable dense β phase.

In particular membranes exhibiting the thermodynamically stable and dense β phase present a proton conductivity which is essentially unaffected by oxidative stability Fenton tests.

Thermogravimetric measurements have also shown that the thermal stability of sulfonated membranes is comparable and even higher than that of unsulfonated films.

Chapter 4 Sulfonated nanoporous s-PS aerogels

The idea to obtain aerogels of s-PS exhibiting the δ nanoporus crystal form and the sulfonated amorphous phase (sulfonated δ-aerogels) arises from the facts that sPS aerogel morphologies have VOCs sorption kinetics much faster than corresponding film morphologies.

In particular, in a recent paper, the apparent diffusivity of DCE (estimated from line slopes in Fick's plots) absorbed from 100 ppm aqueous solutions, in nanoporous s-PS aerogels having a porosity P=98.5%, is nearly 7 order of magnitude larger than the diffusivity in nanoporous s-PS films[29].

Furthermore in a recent work has been shown that the sulfonated s-PS δ-form films present VOCs sorption kinetics from diluted aqueous solution faster than corresponding unsulfonated films[38a].

The sulfonation procedure, as already described in chapter 3, makes hydrophilic the polymer amorphous phase and allows a direct contact between the water containing VOCs and the absorbing s-PS nanoporous crystalline phase.

Based on these previously studies it was easy to assume that the sorption kinetics, from diluted aqueous solutions of VOC pollutants in sPS aerogels with nanoporous crystalline phases, would be further increased sulfonating the s-PS amorphous phase .

In this chapter we described the sulfonation procedure of sPS nanoporous aerogels and their sorption behavior from dilute DCE aqueous solutions.

4.1. Sulfonation procedure

As well as in the sulfonation of sPS films, even in the sulfonation of sPS δ-aerogels the reaction of sulfonation was carried out in heterogeneous phase.

The polymer gels were treated with a solution of an appropriate previously prepared sulfonating agent in chloroform. That solvent is capable of forming a co-crystalline structure with the s-PS nanoporous δ form.

This technique exploits the molecular selectivity of nanoporous δ phase of s-PS. In fact the sulfonating agent, being particularly bulky, can not enter into the polymer crystalline phase so only the amorphous phase benzene rings are sulfonated. At the same time the chloroform solvent, easily penetrates both into amorphous phase and into the nanoporous crystalline phase so the whole polymer is easy and rapidly swelled. The polymer swelling facilities the penetration of sulfonating agent making uniform the sulfonation of the amorphous phase.

The sulfonating reagent, used for the preparation of sulfonated δ-aerogels, as already mentioned above, was acyl sulfate. This reagent was prepared by mixing an excess of dodecanoic acid (lauric acid) over chlorosulfonic acid ($ClSO_3H$) at room temperature. In particular, 1.6 mol of lauric acid were used per 1.0 mol of $ClSO_3H$.

The sulfonation of s-PS was carried out on sPS chloroform gels. In particular the polymer gels were dipped in a solution of acyl sulfate for different time (that time is called "swelling time" in the text).

Then the sulfonation reaction was activated at temperature of 40°C, at different times according to the desired sulfonation degree.

After this, in order to remove the unreacted chemicals, the sulfonated sPS gels were washed repeatedly with fresh chloroform.

Finally solvent extraction with supercritical CO_2 was done to obtain the sulfonated δ-aerogels.

4.1.1 Optimization of sulfonation procedure

In order to obtain s-PS δ-aerogels with different sulfonation degrees, reactions were performed by varying both the concentration of the sulfonating reagent solution and the reaction time

In the **table 4.1**. the experimental conditions of some preliminary tests carried out on sPS gels for optimizing the swelling time are reported

Sample	Reaction time (h)	Swelling time (h)	Concentration (M)	% S atoms/styrenic units[a]
1	72	-	0.05	-
2	4	-	0.1	-
3	8	-	0.1	2
4	1	14	0.05	5
5	1	20	0.05	4
6	1	24	0.05	5
7	1	12	0.1	6
8	1	24	0.1	14

Table 4.1: results of experimental tests carried out for obtain s-PS δ-aerogels with different sulfonation degree. [a]Determinate by elemental analysis.

From the data reported in **table 4.1** can be observed that sulfonation reaction does not occur in the absence of swelling also for long reaction times.

In the absence of swelling, low sulfonation degrees are obtained with higher sulfonating agent concentrations and for long reaction times. Instead for the swelling times greater than 14 hours the sulfonation reaction occurs, even at low concentrations of the sulfonating agent

However the results, reported in table above, clearly show the importance of swelling operation, in fact its absence in sulfonation procedure against δ-aerogels, adversely affect the success of the reaction.

Fixed the time of swelling at 24 h, then the reaction time and concentrations were optimized

In the **table 4.2.** the results in the optimization tests are shown.

Sample	Reaction time (min)	Concentration (M)	% S atoms/styrenic units
1	60	0.05	1.3
2	60	0.1	5
3	120	0.1	14
4	120	0.15	24
5	60	0.2	12
6	60	0.25	31
7	30	0.5	16
8	15	0.5	7.5
9	60	0.5	46

Table 4.2: *sulfonation degree (determined by elemental analysis) of some naoporous δ s-PS film achieved in different sulfonation conditions.*

4.2.2. FTIR characterization

Infrared characterization, even for sulfonated δ-aerogels, gives information about sulfonation degree and allows us to evaluate the crystallinity of polymer samples. In **figure 4.1**. the FTIR spectra, in the region 1450-1420 cm^{-1}, of some δ-form s-PS aerogels at different sulfonation degree are shown.
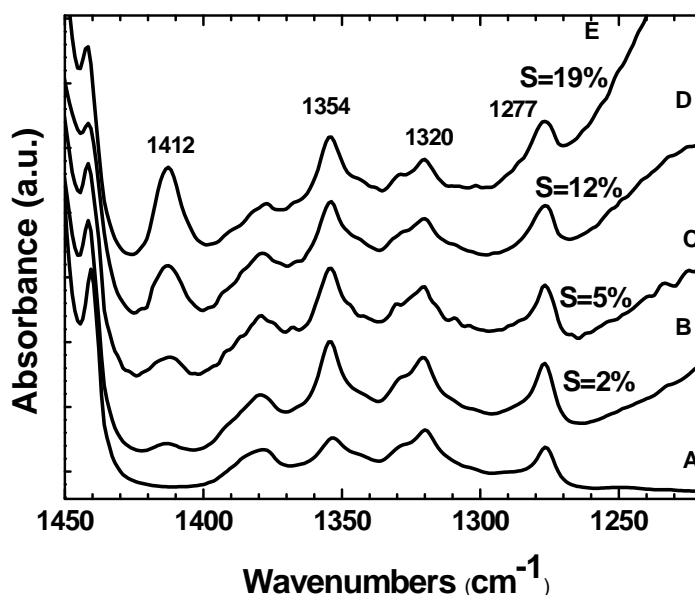
Figure 4.1. FTIR spectra in the wavenumber range 1450-1250 cm^{-1} of s-PS aerogel with nanoporous crystalline δ-phase, (A) before and (B-E) after sulfonation procedures. Relevant absorbance peaks associated with the crystalline (1354, 1320) phase or with the sulfonation level (1412 cm^{-1}) are also indicate.

In this figure the FTIR spectra of sulfonated δ-aerogels, with different sulfonation degree are reported. The progressive increase of the intensity peak at 1412 cm^{-1} is clearly evident.

In **figure 4.1.** the typical peaks of δ crystalline phase, that are located at 1354, 1320 and 1277 cm^{-1} are also shown. The presence

of these peaks is a clear evidence that, after sulfonation, the integrity of δ-crystalline phase of aerogels is preserved.

A linear relationship between the value of sulfonation degree, determined by elemental analysis, and the value of the intensity of the 1412 cm^{-1} peak, is observed. For this reason the FTIR becomes the primary technique for determining sulfonation degree of sulfonated δ-aerogels as well as sulfonated sPS films.

4.2.2. X-ray Characterization

The X-ray analysis allows us to obtain qualitative information about of δ-phase crystallinity.

In **figure 4.2.** the X-ray diffraction pattern of some sulfonate δ-aerogels, at different sulfonation degree are shown.
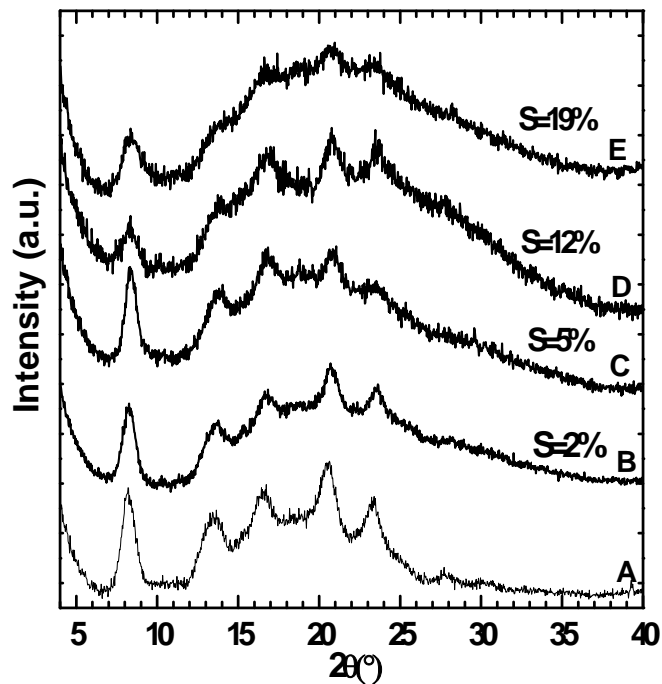
Figure 4.2: X-ray diffraction patterns (Cu Kα) of s-PS aerogels with the nanoporous crystalline δ-phase, (A) before and (B-E) after sulfonation procedures

The X-Ray diffraction patterns show the typical peaks of the nanoporous δ phase. A progressive increase of the intensity of the amorphous halo increasing with the sulfonation degree, is observable in the **figure 4.2**.

However, the position and the intensity of the typical peaks of the nanoporous δ form clearly show that the nature of crystalline phase is essentially unaffected by sulfonation. The broadening of these peaks only indicates a slight reduction of the dimension crystals. As already mentioned for sulfonated nanoporous films, also the sulfonated δ-aerogels retain their dimensional stability even for medium-high sulfonation degree.
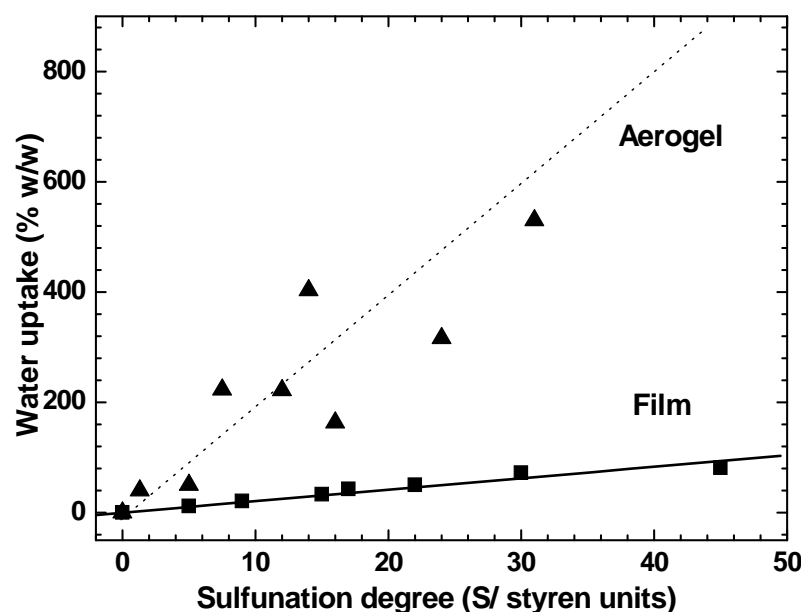
4.2.3. Water uptake

In the **table 4.3.** below the values of liquid sorption water for sulfonted δ-aerogels are reported.

Sample	% S atoms/styrenic units	Water uptake (%ww)
1	1.3	40
2	5	50
3	14	403
4	24	316
5	12	222
6	31	530
7	16	163
8	7.5	223
9	46	1370

Table 4.3.: water uptake of sulfonated δ s-PS aerogels at different sulfonation degree.

In **table 4.3** is clearly evident that the liquid water sorption from sulfonated δ-aerogel already reaches high values at low sulfonation degree.

In this regard, in **figure 4.3.**, we have compared the liquid water sorption behavior of sulfonated δ-aerogels with that of sulfonated δ-films.


Figure 4.3. *Liquid water sorption, as a function of sulfonation degree, from sulfonated films and aerogels of s-PS δ-form.*

Figure 4.3. shows the water uptake *vs* sulfonation degree, for sulfonated s-PS δ-form, in the aerogel and film morphologies.

In **figure 4.3**. the liquid water sorption for the sulfonated films follows a perfectly linear trend, while the data for the aerogels are more scattered. This behavior can be due at the fact that the amount of S determinate by FTIR analysis, for the aerogels, is less accurate because the aerogels absorb too much water.

Anyway the sulfonated δ-aerogels absorb more liquid water than sulfonated films.

Moreover we have evaluated sorption kinetics of water vapor at fixed activity t (a= 0,8) for sulfonated aerogels and films.
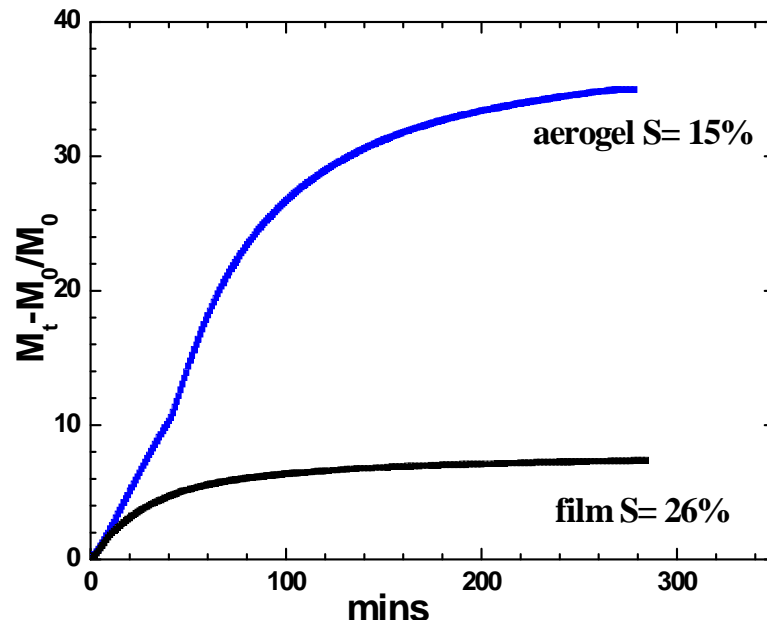
Figure 4.4.: vapor water uptake at room temperature at 0.8 activity, from sulfonated films and aerogels of s-PS δ-form.

In **Figure 4.4.,** an example of water vapor sorption of sulfonated δ-aerogel and δ-film is reported. In the **figure 4.4.** is clearly evident that the sulfonated δ-aerogels absorb much more water vapor than sulfonated films.
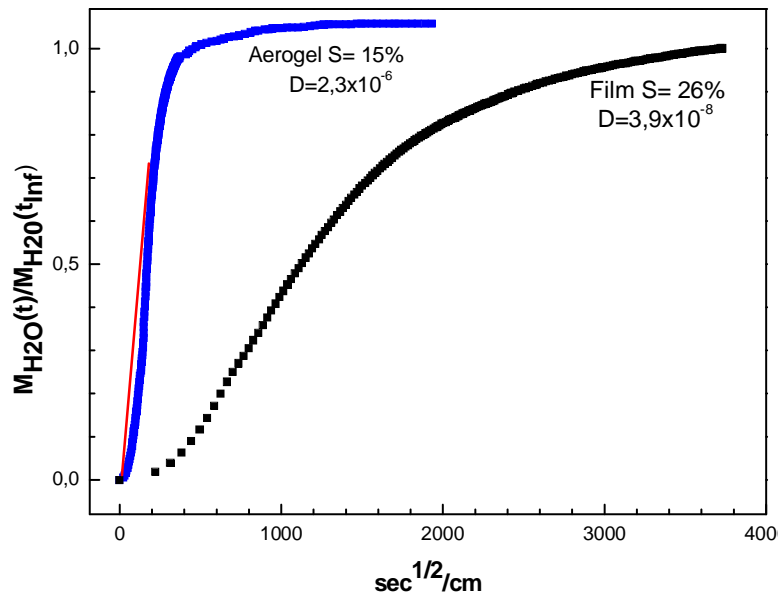
Figure 4.5.: *Sorption kinetics at room temperature of 0.8 water vapor activity, from sulfonated films and aerogels of s-PS δ-form.*

Reporting the sorption time as a function of the time square root, the water vapor sorption kinetics of sulfonated δ-aerogels and film present both a Fick's behavior. Despite the aerogel sample presents a sulfonation degree about half of the film, it absorbs the water vapor faster, in particular the water diffusivity constant (D, reported in **figure 4.5**) for sulfonated δ-aerogel is two orders magnitude larger than that corresponding sulfonated film.

4.3. Sulfonated nanoporous aerogels as absorbent of water pollutants.

In this section we reported the study of the uptake DCE from dilute water solution, at different DCE concentration 50 and 100 ppm, in sulfonated δ-aerogels

The DCE sorption kinetics are obtained by FTIR measurements. In particular the absorbance of the DCE trans conformer of 1234 cm^{-1} was used.
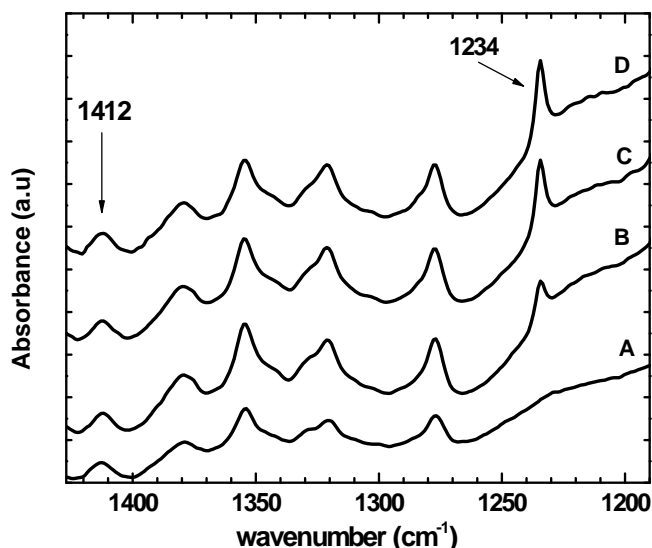
Figure 4.6.: FTIR spectra, in the wavenumber range 1450-1250 cm^{-1}, of sulfonated δ-aerogel with P=90% before (A) and (B-D) with increasing time of DCE sorption from 100 ppm aqueous solution.

Figure 4.6. shows the FTIR spectra of sulfonated δ-aerogel with *P*=90% before (A) and (B-D) after DCE sorption, at different time, from 100 ppm aqueous solution. The increase of the absorbance of trans DCE band at 1234 cm^{-1}, combined with the

absence of the cis DCE band at 1284cm^{-1} [29], suggests that the DCE molecules are only absorbed in δ nanoporous crystalline phase.
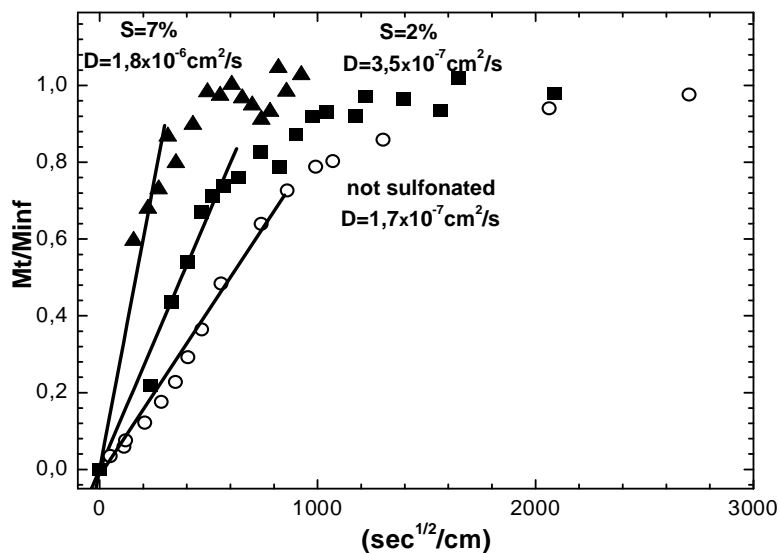
Figure 4.7.: *Sorption kinetics at room temperature of DCE from 100 ppm aqueous solutions, based on the absorbance of its 1234 cm^{-1} trans peak, for δ-form s-PS aerogels at P=90% presenting different degrees of sulfonation of the amorphous phase: not sulfonated; S = 2% andS=7%*

In **figure 4.7.** the comparison of DCE sorption kinetics, from 100 ppm water solution, for two s-PS δ-aerogels at P=90% presenting different sulfonation degrees with the unsolfonated aerogel is shown.

M_t is the amount of penetrant absorbed at time *t*, M_{inf} is the amount of penetrant absorbed at equilibrium, and L is the macroscopic thickness of aerogel.

We can clearly observe that the apparent diffusivities (D) obtained by the slopes of the lines substantially increase with the degree of sulfonation

In particular for the aerogel with only a degree of sulfonation S=7% there is an increase in DCE sorption diffusivity of more than a magnitude order than unsulfonated aerogel.

In **figure 4.8.** the Fick's plot, for DCE sorption from 50 ppm aqueous solutions in two aerogel samples presenting the δ-nanoporous crystalline phase and different sulfonation degrees, are shown.
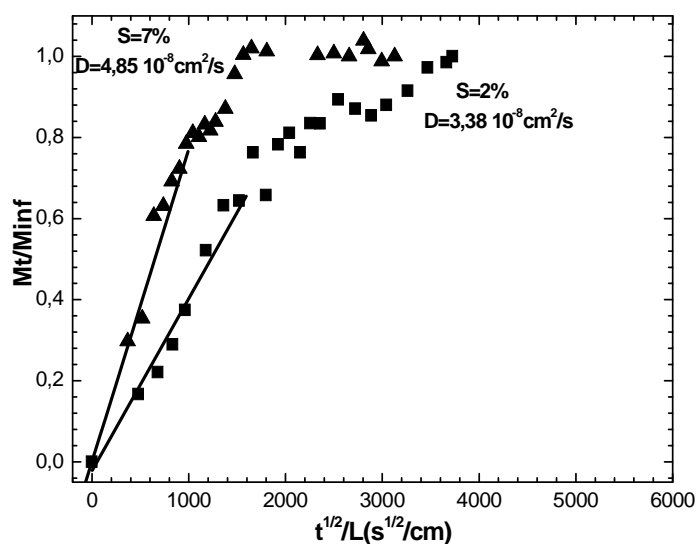
Figure 4.8.: *Sorption kinetics at room temperature of DCE from 50 ppm aqueous solutions, based on the absorbance of its 1234 cm^{-1} trans peak, for δ-form s-PS aerogels at P=90% presenting different degrees of sulfonation of the amorphous phase.*

We can clearly observed, even in this case, that the apparent diffusivities (D) obtained by the slopes of the lines substantially increase with the degree of sulfonation.
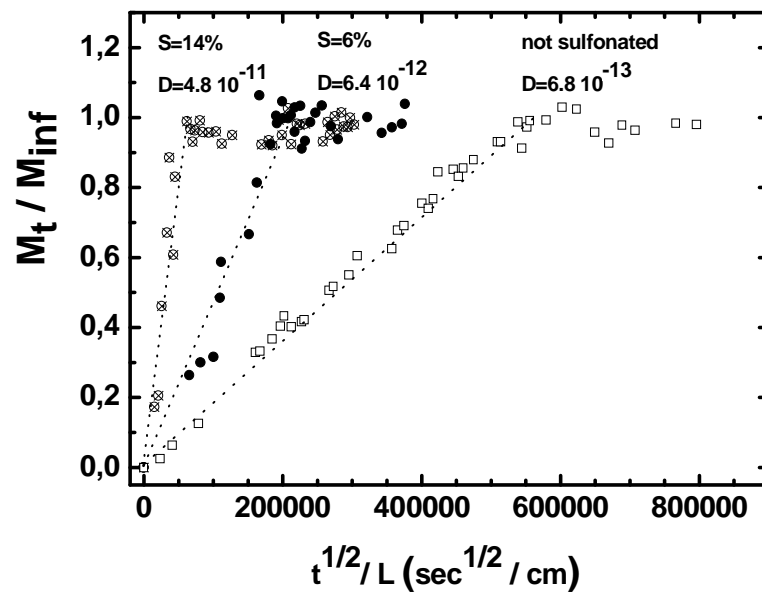
In **figure 4.9** the Fick's plot, for DCE sorption from 50 ppm aqueous solutions in sPS film samples presenting the δ-nanoporous crystalline phase and different sulfonation degrees, are shown.

Figure 4.9.: Sorption kinetics at room temperature of DCE from 50 ppm DCE aqueous solutions, based on the its absorbance of 1234 cm^{-1} trans peak, for δ-form s-PS films presenting different sulfonation degrees of the amorphous phase.

The **figure 4.9**. clearly shows that apparent diffusivities (D) obtained by the slopes of the lines substantially increase with the degree of sulfonation. In particular, for the film with a degree of

sulfonation S=14%, there is an increase in DCE sorption diffusivity of more than 70 times.

However, comparing the values of the apparent diffusivity (D), corresponding at DCE sorption from 50 ppm water solution, for sulfonated films and aerogels in δ-form can be observe clearly that for the latter DCE uptake in sulfonated δ-aerogels are much faster than that observed for sulfonated films.

In **table 4.4**. the difference of the apparent diffusivity (D),determinate by Fick's low for DCE sorption in film and aerogel of s-PS are summarized.

It worth noting that DCE equilibrium uptake, from 100 ppm aqueous solution is nearly independent of the sulfonation degree and not far from 7%.

Sample δ-form s-PS	% S	[DCE]ppm	$D(cm^2/s)$
Unsulfonated film	-	50	$6,8*10^{-13}$
Sulfonated film	6	50	$6,4*10^{-12}$
Sulfonated film	14	50	$4,8*10^{-11}$
Sulfonated aerogel	7	50	$1,2*10^{-8}$
Unsulfonated aerogel	-	100	$1,7*10^{-7}$
Sulfonated aerogel	7	100	$1,2*10^{-6}$

Table 4.4.:comparison of values of apparent diffusiviity (D) for nanoporous s-PS aerogels a films.

4.4. Conclusions

In this chapter we have presented a solid-state sulfonation that allows to achieved sulfonated δ-aerogels. As well as for sulfonated films, the high sulfonation degree makes the amorphous phase highly hydrophilic.

Sulfonating procedure is conducted so that δ crystalline phase is preserved, as well as the dimensional stability of manufactures. In fact X-ray diffraction an Fourier Transform Infrared measurements clearly show that this sulfonation procedure preserve the nanoporous δ-phase and its degree of crystallinity in aerogels.

Sulfonated δ-aerogels present sorption kinetics of DCE from dilute water solution higher than those of the corresponding unsulfonated aerogels, which are already extremely fast in removal of VOC from water. For instance, DCE sorption kinetics from 100 ppm solutions, measured for aerogel with a sulfonation degree of S = 7% with a porosity P=90 % show sorption diffusivity of more than a magnitude order higher than corresponding unsulfonated aerogel.

Moreover is easly predictable that sulfonated δ-aerogels absorb more water (liquid and vapor) and faster than nanoporous sulfonated films.

These results indicate that sulfonated aerogels whit δ-form crystalline phase can be particularly suitable to remove VOC pollutants from water and moist air.

Chapter 5 : Chloromethylation of polystyrene

In this chapter is described the chloromethylation of s-PS. The idea to obtain the chloromethylated s-PS arises from the fact that the corresponding non-crystalline polymer, atactic chloromethylated polystyrene (aPS) [44]-[45], is a polymer of remarkable commercial importance. It was obtained, from Merriefield, for the first time, in 1963 [43]. Moreover, the introduction of a chloromethyl group, on the aromatic ring makes the polymer further functionalizing by simple nucleophilic substitution reactions with other reagents.

The approach used for the chloromethylation of s-PS was the same utilized for the sulfonation. In particular, even in this case the procedure involves reactions in heterogeneous phase.

Since the chloromethylation procedure of s-PS is not reported in the literature, in order to test the procedure and identify the most suitable reaction conditions, the reaction has been previously tested on atactic polystyrene. This non-crystalline polymer is easily soluble in organic solvents whose characteristics are known.

The chloromethylation of aPS is called, in the text, "model reaction".

In scheme 5.1 is reported the chlorometylation reaction as carried out in this work.
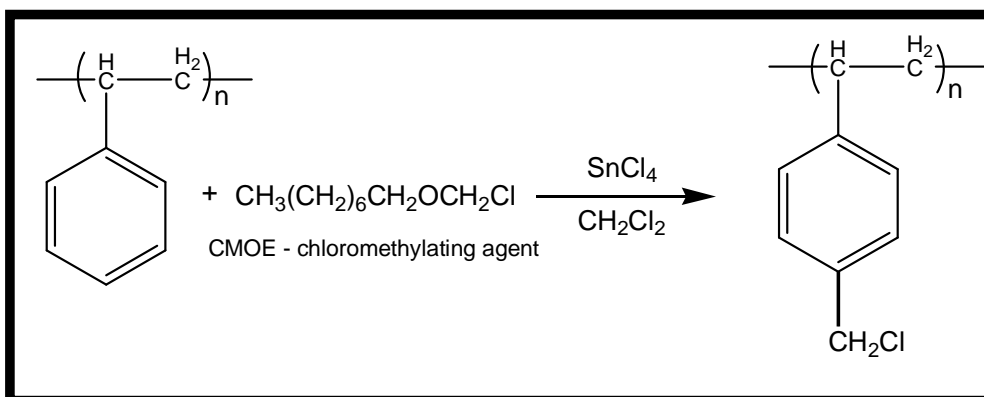
Scheme 5.1.: *Chloromethylation reaction*

5.1. Model reaction: chloromethylation of a-PS

5.1.1 Chloromethylation procedure

The reaction model was carried out in solution, the introduction of chloromethyl-groups as substituent of polymer aromatic nuclei, is performed by treating the polymer with chloromethyloctylether, (CMOE) bulky reagent.

The Friedel-Craft catalyst for the chloromethylation was $SnCl_4$ and dichloromethane was solvent. In particular the chloromethylation process is divided into the following steps:

1. the pellets of a-PS that were dissolved in CH_2Cl_2 (anhydrous) at room temperature in a flask
2. CMOE(anhydrous) was added

73

3. SnCl$_4$was added (anhydrous), in dry box

4. the flask was immersed into an oil bath at 40°C and left, under stirring 24 h in dark, for the completion of the reaction.

All the operation, above described, were carried out under inert atmosphere with N$_2$.

At the end of the reaction, the polymer solution was precipitated in methanol, filtered and dried at room temperature. In order to remove the excess of the unreacted chemicals, the produced polymer was dissolved again in chloroform, precipitated in methanol, filtrated and dried at room temperature.

This purification procedure was repeated for three times. The chloromethylated polymer was stored in dark at low temperature to avoid polymer cross-linking.

5.1.2. NMR Analysis

In order to confirm that the chloromethylation reaction has been successful, the product of reaction model (chloromethylated a-PS called CMaPS in text) was analyzed by NMR and the result are reported in **figure 5.1**.
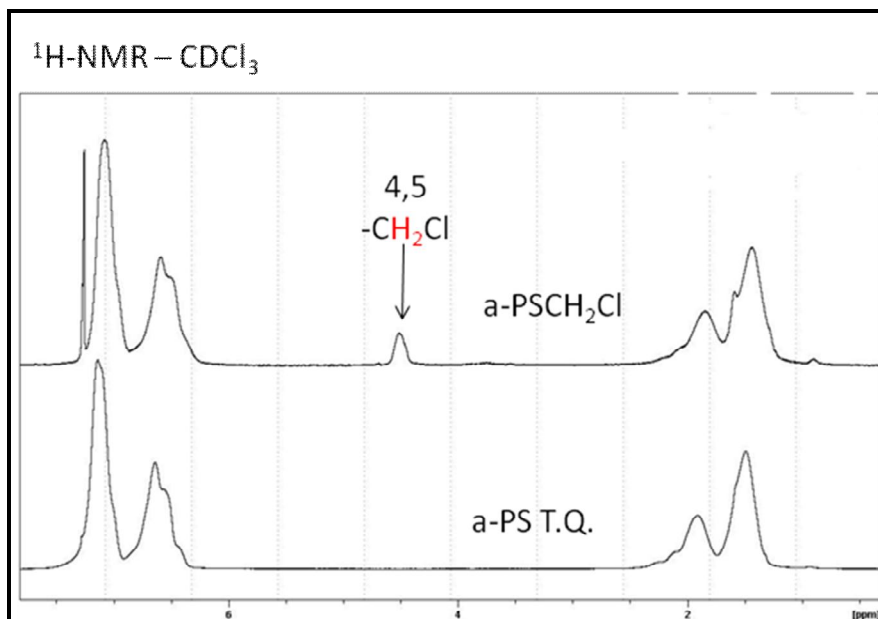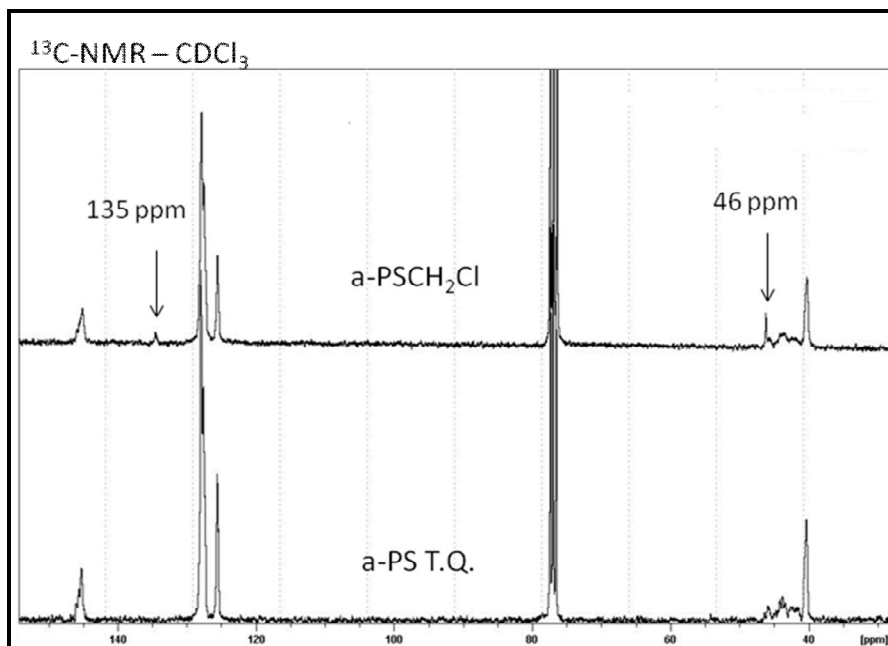
Figure 5.1.: *¹H-NMR spectra of a-PS before (a) and after (b) chloromethylation procedure*

In the **figure 5.1** is reported the comparison of the ¹HNMR spectra for a-PS before and after chloromethylation. In **figure 5.1b** the new peak observed at 4.5 ppm can be certainly associated to the methylene protons of the chloromethyl groups, which was absent in the ¹HNMR spectrum of a-PS as it is. The presence of the chloromethyl groups on phenyl ring of a-PS don't seem to alter other typical signals of the polymer.

Moreover in **figure 5.2** the comparison of ¹³CNMR spectra for a-PS before and after chloromethylation procedure is reported.

Figure 5.2.: ^{13}C-NMR spectra of a-PS before (a) and after (b) chloromethylation procedure

In **figure 5.2b** the new peak at 135 ppm can be associated to the quaternary aromatic carbon bonded to the chloromethyl groups. New peak at about 46 ppm can be associated to methylene carbon which is very close to broad signals of the aliphatic carbons chain

The results obtained by NMR analysis clearly confirm that the chloromethylation procedure for model reaction has been successful.

5.1.3 FTIR analysis

Infrared analysis of CMaPS allows us to obtain information about the chemical modifications, in particular it can provide information on the success of the reaction.

In **figure 5.3** the FTIR spectrum of CMaPS are reported, in particular the area between 1700 e 800 cm^{-1} is shown.
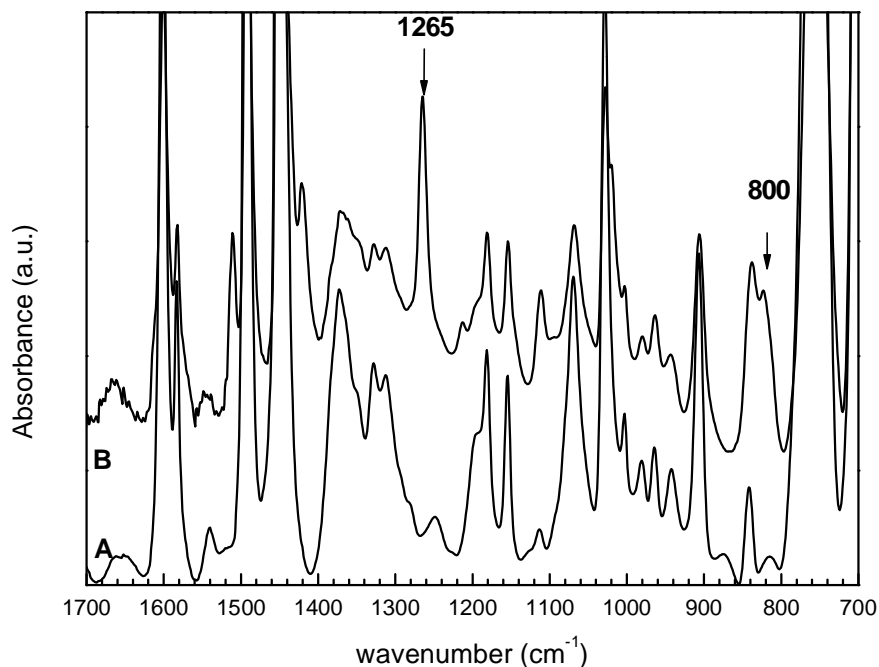
Figure 5.3.: *FTIR spectra in the wavenumber range 1700-700 cm^{-1} of a-PS samples. (A) before and (B) after chloromethylation procedures. Relevant absorbance peaks associated the chloromethylation level (1265-800 cm^{-1}) are indicate.*

In **figure 5.3** after chloromethylation a-PS, two new peaks, at 1265 cm^{-1} and 800 cm^{-1} can be ascribed to the -CH$_2$Cl group. This peak indicates that the polymer has been successfully chloromethylated with the procedure above described.

5.2. Chloromethylation of syndiotactic polystyrene

5.2.1. Chloromethylation procedure

The δ-form films subjected to the chloromethylation procedure have been obtained by casting from 0.5 wt% solutions in chloroform, at room temperature.[14] The films present uniplanar orientation of δ-nanoporous and co-crystalline phases and thickness in the range 40-60 μm.

As already mentioned above the approach used in the chloromethylation of s-PS was the same utilized in the sulfonation procedure.

In particular, even in this case, the technique involves a reaction in heterogeneous phase, the use of solvents capable of forming co-crystalline structures of s-PS, and an appropriate chloromethylating agent.

This technique exploits the molecular selectivity of nanoporous δ phase of s-PS. In fact the chloromethylating agent, being particularly bulky, can not enter into the polymer crystalline phase so only the amorphous phase benzene rings are chloromethylated. At the same time the solvent, easily penetrates both into amorphous phase and into the nanoporous crystalline phase so the whole polymer is easy and rapidly swelled. The polymer swelling facilities the penetration of chloromethylating agent making uniform the chloromethylation of the amorphous phase.

The reaction of the sPS was performed using the same procedure developed for the reaction model, but adjusting it in heterogeneous phase.

The introduction of chloromethyl-groups as substituent of aromatic nuclei, in amorphous phase is performed by treating the polymer with chloromethyloctylether, (CMOE) bulky reagent.

The Friedel-Craft catalyst for the chloromethylation was $SnCl_4$ and dichloromethane was solvent. As well as for chloroform, in the sulfonation procedure, the dichloromethane is capable to swell the polymer and to form co-crystalline structure with the host nanoporous crystalline δ form of s-PS.

In particular the chloromethylation process of s-PS is divided into the following steps:

1. the s-PS δ-films were dipped in a flask containing a solution of CMOE in CH_2Cl_2 and them swelled for 3 h (during this time the reagent penetrates throughout the bulk to film.

2. $SnCl_4$was added (anhydrous) and so the heterogeneous system was left to swell for one hour, (during this time the catalyst penetrates throughout the bulk to film)

3. the flask was immersed into a oil bath at 40°C and left, 24 h in dark, for the completion of the reaction.

All the operation, above described, were carried out under inert atmosphere with N_2.

At the end of the reaction, the s-PS film was taken out of the flask and washed, repeatedly, with fresh chloroform. in order to remove the excess of the unreacted chemicals.

The s-PS chloromethyled film (CMsPS) obtained was stored in dark and at low temperature to avoid polymer cross-linking.

In order to obtain polymer samples with different content of chloromethyl groups, a series of tests were carried out by varying the concentration of the chloromethylating reagent.

In the **table 5.1.** the chloromethylation degree, determined by the elemental analysis, for the various chloromethilated samples have been reported with the ratio of moles of CMOE and the moles of styrene units present in the amount of polymer used

Sample	mol CMOE/mol s-PS	% Cl atoms/styrenic units
1	4:1	13,5
2	5:1	9,9
3	2,3:1	7,7
4	3:1	7,6
5	2:1	6,9
6	1,5:1	5,1
7	1:1	3,7

Table 5.1.: chloromethylation degree (determined by elemental analysis) of some nanoporous δ s-PS film achieved with different ratio ratio of moles of CMOE and the moles of styrene units present in the amount of polymer used

From the data reported in the **table 5.1**. can be observed that increasing the concentration of chloromethylating reagent (CMOE) increases the percentage of chlorine in the polymer.

5.3. Characterization of chloromethylated nanoporous s-PS films

5.3.1. FTIR analysis

As well as for CMaPS infrared analysis of CMsPS allows us to obtain information about the chemical modifications, but also about the possible structural changes of polymer induced by the chloromethylation reaction.

In the **figure 5.4.** the comparison between the FTIR spectra of CMsPS and CMaPS is reported. Also for s-PS, after chloromethylation the two new peaks at 1265 e 800 cm^{-1}, ascribed to the CH$_2$Cl group, can be observed. This confirm that the solid-state chloromethylation of s-PS was successful.
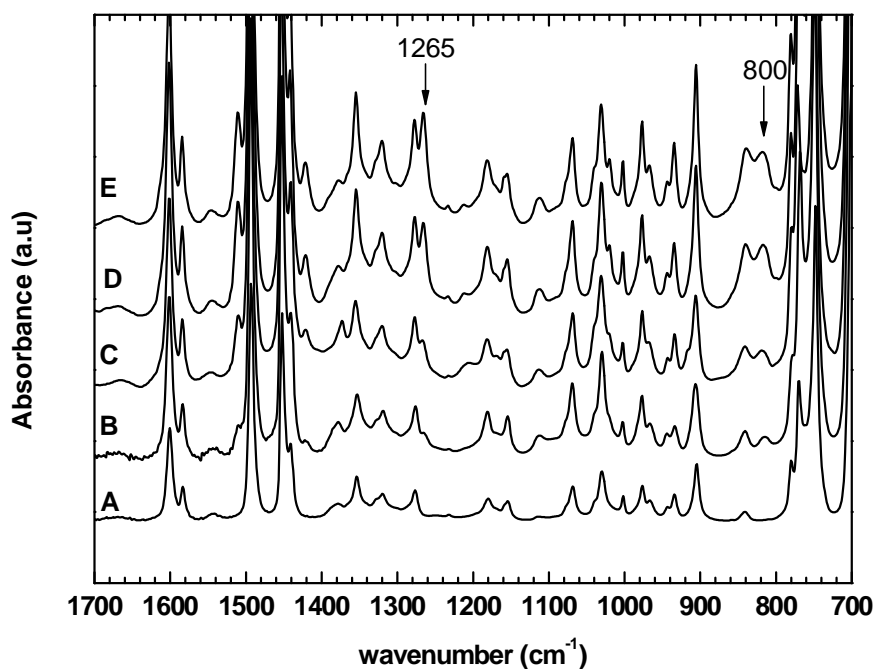
Figure 5.4.: *comparison of the FTIR spectra in the wavenumber range 1700-700 cm^{-1} of a-PS and s-PS samples. (A) before and (B) after chloromethylation procedures. Relevant absorbance peaks associated the chloromethylation level (1265-800 cm^{-1}) are indicate for both chloromrthylated polymer*

Indeed in figure 5.5. the spectra of samples 1,3,5,7 with an amount of chlorine, respectively, 13.5, 7.7, 6.9, 3.7 are reported.

As is clearly evident the intensities of the two peaks at 1265 and 800 attributed to the group CH$_2$Cl increase with increasing chlorine in the polymer.
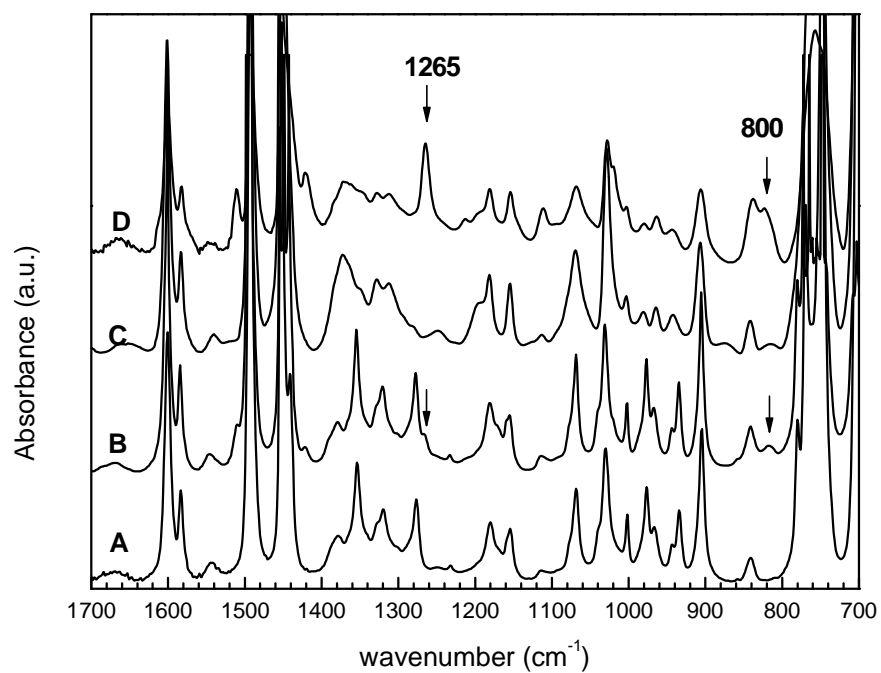
Figure 5.5.: *FTIR spectra in the wavenumber range 1700-700 cm^{-1} of s-PS samples with nanoporous crystalline δ-phase, (A) before and (B-E) after chloromethylation procedures. Relevant absorbance peaks associated with the crystalline (1354, 1320,1277cm^{-1}) phase or with the chloromethylation level (1265, 800 cm^{-1}) are also indicate.*

Moreover is, also, possible to observe the presence of δ-crystalline phase typical peaks, they are located at 1354, 1320 and 1277 cm^{-1}, the presence of these unaltered peaks is a clear evidence that the chloromethylation procedure unaffected the integrity of s-PS films δ-crystalline phase.

5.3.2 X-Ray Analysis

The X-ray analysis allows us to obtain qualitative informations about of crystallinity δ-phase and its orientation in chloromrthylated films.

In **figure 5.6.** the X-ray diffraction patterns of some chloromethylated δ-form s-PS films with a different chloromethylation degree, are shown
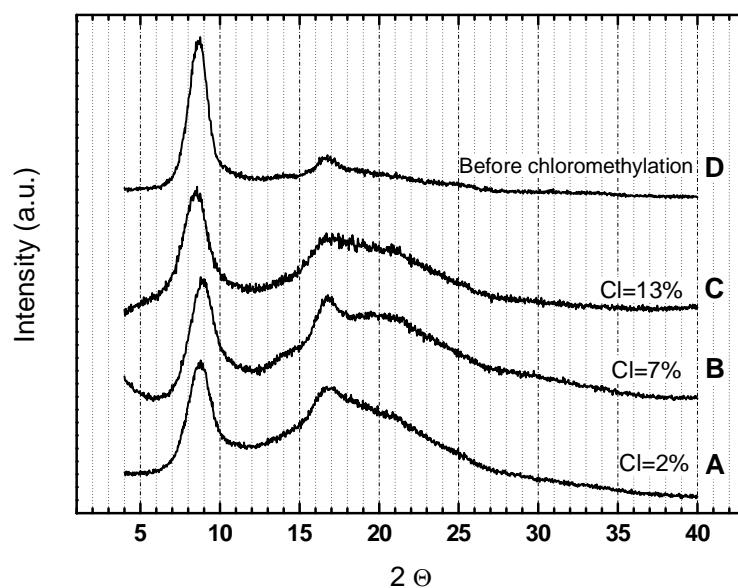
*Figure 5.6.: X-ray diffraction patterns (Cu Kα) of s-PS films with the nanoporous crystalline δ-phase, (A) before and (B-d) after chloromethylation procedures.*

The X-Ray diffraction patterns, show only (010) and (020) reflections, at $2\theta CuK\alpha \approx 8.4°$ and $\approx 17°$ peaks. These peaks are typical the nanoporous δ crystals having a high level of uniplanar orientation.

The position of the peak at $2\theta CuK\alpha \approx 8.4°$ remains essentially unchanged even at high degrees of chloromethylation. However we can observe, a partial broadening of this peak and a decrease in its intensity. This behavior can be rationalized on the basis of a reduction in crystal size and the increase of the diffuse scattering in the amorphous phase due to the presence of heavy atoms of chlorine.

5.3.3. TGA Analysis

In **figure 5.7**. the TGA curves of the δ form film with a chloromethylated amorphous phase (Cl = 9%) has compared with that one of unchloromethylated δ-form film are shown.
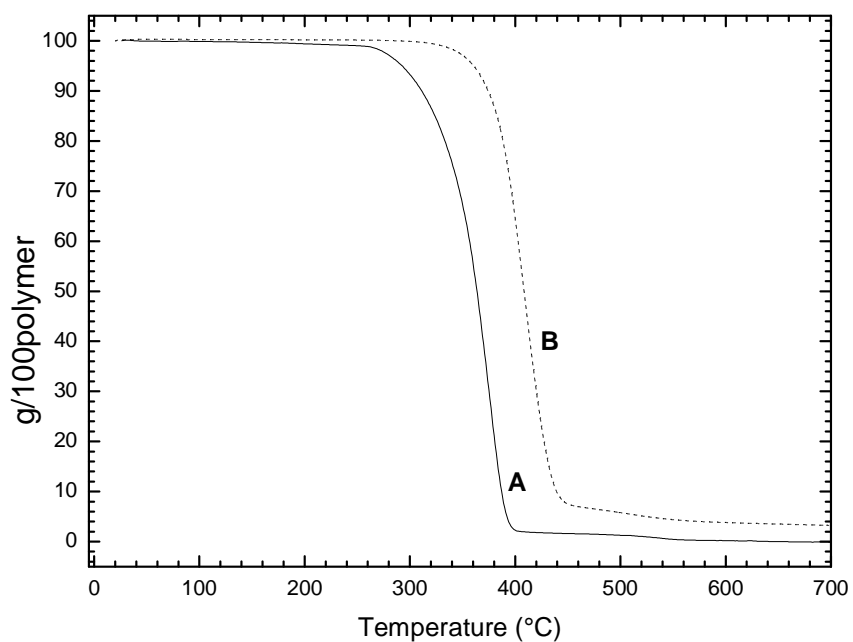
Figure 5.7. *TGA of s-PS δ-crystalline form film:*
(A) unchlorometilated (B) with a chloromethylation degree Cl =9%.

In **figure 5.7.** it is possible to observe that the s-PS chloromethylated δ-form film (B) present a degradation temperature of 50 Celsius degrees higher than the s-PS unchloromethylated film(A).

The higher degradation temperature showed by curve B possibly corresponding to a partial cross-linking degree present in the chloromethylated polymer sample.

5.4. Chloromethylated s-PS as starting material for other functionalized polymers

In order to extend the possibilities to use functionalized s-PS as PEM the introduction of a positive charged group on the polymeric chain was achieved by a reaction between the chloromethylated s-PS (described above) and a tertiary amine.

In this section the best result obtained after a series of reaction attempts is shown, in particular is described the amination of CMsPS with a chloromethylation degree of 7%.

5.4.1 Amination procedure
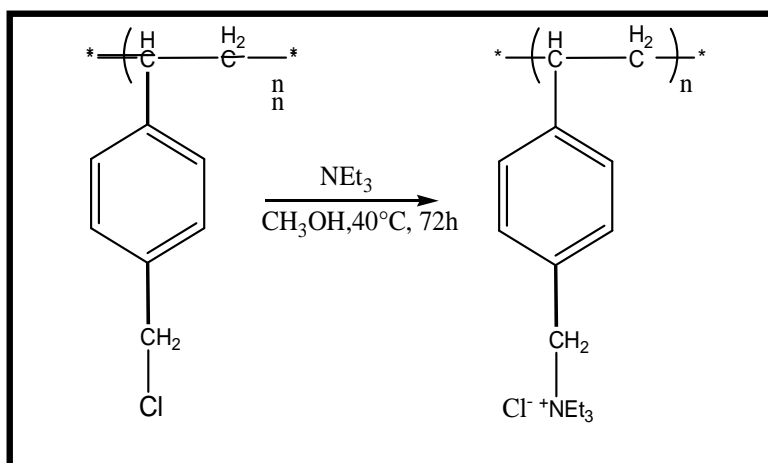
Scheme 5.2.: *Amination reaction*

The approach used in this reaction is the same used in sulfonation and chloromethylation procedures described in previous chapters. The solid-state reaction was carried out directly on the chloromethylated film samples.

The adopted amination technique takes as reference to a procedure recently reported in the literature [46] and is divided into the following steps:

- The chloromethylated film was dipped in a flask containing a solution (1M) of triethylamine in methanol.
- The film was left into a solution for 24 h to swell
- The flask was immersed in an oil bath at 40°C and left them for 72 h to complete the reaction.

At the end of the reaction, the s-PS film was taken out of the flask and washed, repeatedly, with water in order to remove the excess of triethylamine.

5.4.2. FTIR analysis of aminated s-PS film

Infrared analysis of aminated s-PS allows us to obtain information about the chemical modifications, but also about the possible structural changes of polymer induced by the amination reaction.

In the **figure 5.8.** the comparison between the FTIR spectra of CMsPS (Cl = 7%) and aminated s-PS is reported. After amination of peak at 1265 cm^{-1} ascribed to the CH$_2$Cl group disappears, while the presence of two new peaks at 1666 e 1381 cm^{-1}, ascribed to the NEt$_3$ group is observed; this is a clear demonstration that amination reaction was successful.
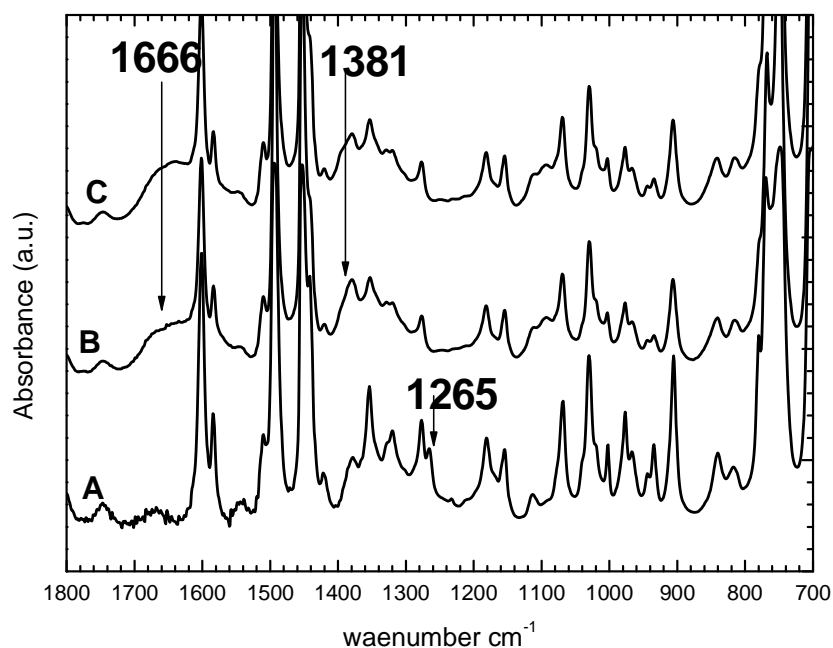
Figure 5.8.: *FTIR spectra in the wavenumber range 1700-700 cm^{-1} of s-PS samples with nanoporous crystalline δ-phase, (A) chloromethylated s-PS, (B) after amination procedure and (C) after cleaning with water . Relevant absorbance peaks at 1265 cm^{-1} ascribed at chloromethyl group and at 1381 and 1666 cm^{-1} ascribed at triethylamine group are indicate.*

Moreover is also possible to observe the presence of δ-crystalline phase typical peaks, they are located at 1354, 1320 and 1277 cm^{-1}, the presence of these peaks is a clear evidence that the amination procedure unaffects the integrity of s-PS films δ-crystalline phase.

5.4.3. X-Ray Analysis of aminated s-PS film

The X-ray analysis allows us to obtain qualitative informations about δ-phase crystallinity and its orientation (010) in aminated s-PS films.

In **figure 5.9.** the comparison of X-ray diffraction patterns between CMs-PS films and aminated s-PS, is shown.
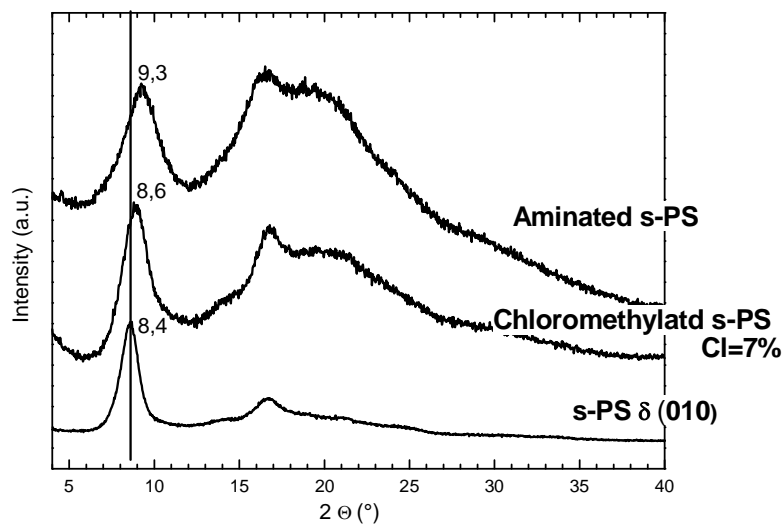
Figure 5.9.: *X-ray diffraction patterns (Cu Kα) of s-PS films (A) with the nanoporous crystalline δ-phase before chloromethylation, (B) after chloromethylation procedures and (C) after amination procedure..*

The X-Ray diffraction patterns, show only (010) and (020) reflections, at $2\theta CuK\alpha \approx 8.4°$ and $\approx 17°$ peaks. These peaks are typical the nanoporous δ crystals having a high level of uniplanar orientation.

The position of the peak at $2\theta CuK\alpha \approx 8.6°$, after amination procedure is shifted at $2\theta CuK\alpha \approx 9.3$. Furthermore, in the spectrum

of aminated s-PS the broadening of the peak, probably due to the reduction of crystal size and the increase of the diffuse scattering in the amorphous phase, can be observed.

For the aminated s-PS sample above described was evaluated the water uptake and the anionic conductivity. In particular it show water uptake of 21% at which correspond low value of anionic conductivity, it is about 5 mS at 30 °C.

5.5. Conclusions

In this chapter we have presented a novel solid-state chloromethylation procedure, which when applied to syndiotactic polystyrene samples exhibiting the nonporous δ-crystalline phase allows an easy and uniform chloromethylation of the phenyl rings of the amorphous phase.

The chloromethylation procedure and better conditions at which carried out it were tested, preliminarily by the reaction model.

The reaction model was carried out on aPS and provides a chloromethytation procedure carried out in solution.

The successful of reaction model was confirmed by NMR and FTIR analysis of choromethylated polymer obtained

Indeed X-ray diffraction and Fourier Transform Infrared measurements on chloromethylated s-PS δ-form films clearly show that the proposed chloromethylation procedure is able to preserve nanoporous δ-phase, essentially also preserving its degree of crystallinity.

Moreover the chloromethylation procedure was optimized so we were able to modulate the chloromethylation degree of s-PS films in according our needs.

Finally the CMsPS was utilized as starting material for other functionalized polymer, in fact was proposed the amination reaction, in order to obtain PEM characterized by anionic conductivity, that was successful.

Bibliografia

[1] M.K. Mishara *Polymer Frontieres International* **1994**

[2] J.R. Ebdon New mwthods of Polymer Synthesis Blacker and Sons, New York, **1991**

[3] Y.Yagci; M. Mishara Handbook of Vinyl Polymers: Radical Polymerization and Technology

[4] (a) M. Okawara, K. Dojin, **1972** . (b) Y. Iwakura; K. Kurita, **1977**

[5] (a) R. Kumin, R.E. Krieger; *Pub. Comm.* **1972**; (b) H. Hisayama *Ion Exchange Resins*, **1976**.

[6] L.M. Minsk, J.G. Smith, W.O. Van Densen, J.F. Write, J.App.Polym. Sci. 2:302; **1959**.

[7] T. Nishikubo Polymer reactions for the Synthesis of Functional Polymers.

[8] M.A. Grauthier, M.I. Gibson, H-A. Klok, *Angew, Chem. Int. Ed.*48-58, **2009**

[9] N. Ishiara, T. Scimiya, M. Kuramoto, M. Hoi, Macromolecules; 19:2464, **1986**.

[10] R.Po, N. cardi, *Prog. Polym. Sci.* 21:47, **1996**.

[11] N. Tomotsu, N. Ishihara, T.H. Newmann, M.T Malanga, *J. Mol. Catal.* 128:167, **1998**.

[12] M.T Malanga, *Adv. Mater.* 12:1869, **2000**.

[13] J. Schellenberg, N. Tomotsu, *Prog. Polym. Sci.*27:1925, **2002**.

[14] S.D. Amin, T.S. Marks, *Angew. Chem.*, 47:2, **2008**.

[15] (a) F. De Candia, A.Filtro, V.Vittoria, *Macromol. Rapid. Comm.* 23:1335, **1991**; (b) V. Petraccone, F. Auriemma, F. Dal

Progetto, C. De Rosa, G. Guerra, C. Manfredi, P Corradini, *Macromolecules*, 26:3772, **1993**.

[16] (a) C. De Rosa, G. Guerra, V. Petraccone, P. Corradini, *Polym. J.* **1991**, 23, 1435 (b) L. Cartier, T. Okihara, B. Lotz, *Macromolecules* **1998**, 31, 3303 (c) C. De Rosa, *Macromolecules* **1996**, 29, 8460.

[17] (a) C. De Rosa, M. Rapacciuolo, G. Guerra, V. Petraccone, P. Corradini, *Polymer* **1992**, 33, (b) Y. Chatani, Y. Shimane, T. Inagaki, H. Shimane, *Polymer* **1993**, 34, 4841.

[18] (a) G. Guerra, V.M. Vitagliano, C. De Rosa, V. Petraccone, P. Corradini, *Macromolecules* **1990**, 23, 1539, (b) C. Manfredi, C. De Rosa, G. Guerra, M. Rapacciuolo, F. Auriemma, P. Corradini, *Macromol. Chem. Phis.* **1995**, 196, 2795. (c) Rizzo, P.; Lamberti, M.; Albunia, A. R.; Ruiz de Ballesteros , O.; Guerra, G. *Macromolecules* **2002**, 35, 5854

[19] O. Tarallo, V. Petraccone, V. Venditto, G. Guerra, *Polymer* **2006,** 47, 2402

[20] De Rosa, G. Guerra, V. Petraccone, B. Pirozzi, *Macromolecules* **1997**, 30, 4147

[21] A. Immirzi, F de Candia, P. Iannelli, V. Vittoria, A. Zambelli, *Makromol. Chem. Commun.* **1988,** 9, 761

[22] G. Mensitieri, V. Venditto, G. Guerra, Sensors and Actuators **2003**, 92, 255.

[23] O. Tarallo, V, Petraccone, A R. Albunia, C Daniel, G Guerra, Macromolecules, **2010**, 43, 8549.

[24] S.S. Kistler, *Nature*, **1931**, 127, 741.

[25] H.D. Gesser, P.C. Goswami, *Chem. Rew.* **1989**, 89, 765.

[26] (a) Daniel, C.; Alfano, D.; Venditto, V.; Cardea, S.; Reverchon, E.; Larobina, D.; Mensitieri, G.; Guerra, G., *Adv. Mater.* 17, 1515, **2005**, (b) Guerra, G.; Mensitieri, G.; Venditto, V.; Reverchon, E.; Daniel, C. Italy, WO 2005012402 2005.

[27] (a) Malik, S.; Rochas, C.; Guenet, J. M., *Macromolecules* 38, 4888,**2005,** (b) Malik, S.; Roizard, D.; Guenet, J. M., *Macromolecules* 39, 5957, **2006.**

[28] C.Daniel, S.Giudice, G.Guerra *Chem.Mater.* **2009**, *21*, 1028

[29] Daniel, C.; Giudice, S.; Guerra, G., *Chem. Mater,* **2008**, 20, 577.

[30] P. Zinck, F. Bonnet, A. Mortreux,M. Visseaux, *Progress in Polymer Science,* **2008**.

[31] Harder S, Feil F, Knoll K. *Angew Chem* , **2001**;40:4261.

[32] Boffa LS, Novak BM. *Chem Rev*, **2000**;100:1479.

[33] Chung TC. *Prog Polym Sci* **2002**;27:39.

[34] Boan NK, Hillmeyer MA. *Chem Soc Rev,* **2005**;34:267.

[35] Dong JY, Hu Y. *Coor Chem Rev* **2006**;250 :47.

[36] Lopez RC, D'Agosto F, Boisson C. *Prog Polym Sci* **2007**;32:419.

[37] (a) E.B. Orler, DJ. Yontz, R.B. Moore, *Macromolecules*, **1993**, 26:5157, (b) Z. Su, X. Li, SL Hsu, *Macromolecules,* 1**994**, 27:287, (c) E. Orler, V. Bruce Gummaraju Raghuram, H. Chaloun Bret, R.B. Moore, *Macromolecules*, **1999**, 32:1180, (d) A. Borriello, M. Lavorgna, N. Malagnino, G. Mensitieri, T. Napoletano, L. Nicolais, *Macromol Symp*, **2004**, 218:293.

[38] (a) A. Borriello, L. Ambrosio, V.Venditto, G. Guerra, It. Pat Appl. Sa2009A000002; **2009**, (b) A. Borriello, P. Agoretti, L.

Ambrosio, G. Fasano, M. Pellegrino, V. Venditto, G. Guerra, *Chem. Mater.,* **2009**:21.

[39] E. Reverchon, G. Guerra, V. Venditto, *J. Appl. Polym. Sci.* **1999**, 74, 2082

[40] (a) SMJ Zaidi, SD Mikhailenko, GP Robertson, MD Guiver, s. Kaliaguine, *J. Membr. Sci*, **2000**; 173:17; (b) JA Kerres, *J. Membr. Sci,* **2001***; 185:3.*

[41] (a) G. Guerra, VM Vitagliano,P. Corradini, E. albitazzi, It. Pat.19588. Himont Inc; **1989**; (b) Rapacciuolo M, De Rosa C, Guerra G, Mensitieri G, Apicella A, Del Nobile MA. J*. Mater. Sci. Lett.* **1991**; 10(8):1084-87.

[42] AB La Conti, M. Hamdan, RC McDonald, Handbook of fuel cell, vol 3, New York: John Wiley & Sons 2003

[43] R.B. Marrefield *Synthesis of tetrapeptide,* **1963**.

[44] N. Bikac,G. Koza, Y. Yagci, *J. Polym. Mater* 8:189, **1991**.

[45] Giffin D. Jones, Industrial and engineering in chemistry Vol. *44,* No. 11.

[46] Faraj M., Elia E., Boccia M., Filpi A., Pucci A., Ciardelli F., *J. of Polymer Sci. Part A: Polymer Chemistry*, 49, 3437-3447, **2011**.

Le donne sono mamme e tante volte anche papa'…
lavorano dentro e fuori casa con non meno fatica
dell'uomo anche se la forza fisica è inferiore… si
sacrificano, accudiscono… amano…soffrono…cadono e
si rialzano…rinascono dopo ogni delusione come solo
loro sanno fare…. Portano la gonna, ma sanno portare
anche i pantaloni!! si fermano a pensare ai problemi ma
allo stesso tempo pensano …